Towards the Design of Biomimetic Dental Implants: Defining the Natural Periodontal Ligament's Structure and a Scoping Review of Soft Tissue Interfaces

Mohamad Alkayyal BDS, SSC-RD, SBRD

Faculty of Dental Medicine and Oral Health Sciences
McGill University, Montreal
December, 2024

A thesis submitted to McGill University in partial fulfillment of the requirements of the degree of Master of Science (Dental Sciences-Thesis)

Table of Contents

Abstract:

Background: Tooth loss is one of the most prevalent oral diseases. Usually, tooth loss is treated either by removable, fixed, or implant-supported prosthesis. While osseointegrated dental implants represent a largely successful treatment option, they still have anatomical, biological, physiological, and mechanical shortcomings. Most of these shortcomings are attributed to the lack of periodontal ligament (PDL) around dental implants. Surprisingly, the literature lacks proper understanding of the PDL due to difficulty in imaging and studying this part in its 3D geometry. It is a clinical necessity to improve treatment for tooth loss by re-establishing the PDL and its associated functions around an implant. Proper understanding of the PDL is paramount to achieving this goal.

Objectives: i) to define the PDL's natural 3D structure while in its anatomical position utilizing contrast enhanced nano-computed tomography imaging and ii) to perform a scoping review of research areas working towards building a biomimetic dental implant or interfaces between implants and investing tissues.

Materials and Methods: C57Bl/6 mice (n=5), aged 28-35 days were euthanized. Ten half-mandible samples were prepared and fixed in Bouin's solution for 24h, then stored in the refrigerator. The samples were stained with either iodine potassium iodide (IKI), phosphotungstic acid (PTA), phosphomolybdic acid (PMA), mercury chloride (HgCl), or no stain. Then, the samples were mounted in agarose before scanning. The Zeiss Xradia 520 versa nano-computed tomography imaging unit was used. Images processing was performed using dragonfly software.

For the scoping review, Medline, Embase, Scopus, and Compendex were searched with the help of a librarian from the McGill University library. Deduplication were completed on endnote. Two blinded reviewers completed the Initial inclusion/exclusion by screening of titles and abstracts using Rayyan. The full text was reviewed in the next stage to reach the final included records. Eligibility criteria included i) English language, ii) biologically induced growth of an attachment between bone and biocompatible implant, iii) scaffold or other engineered construct to act as an interface between bone and biocompatible implant, iv) in-vivo and in-vitro studies.

Results: The PDL was imaged successfully in the stained samples but not the unstained ones. However, the collagen fibers were not visible even after staining. The physical size of the samples should be minimized to reduce total imaging time. Staining time should range from 24h (IKI) to 48h (PTA, PMA, HgCl). PTA and PMA would exhibit the optimum contrast. Scanning parameters should be optimized to maximize contrast and resolution. Proposed parameters are voltage ≅ 40kV, current ≅ 70μA, pixel size $\leq 0.7\mu m$, optical magnification at 10X, and exposure time ≥ 20 seconds.

In the scoping review, the initial stage yielded 9,562 records. After screening of titles, abstracts, and full text, 82 articles satisfied the defined inclusion criteria. The included studies were classified as PDL regeneration (n=77) or PDL substitution (n=5). The studies were also categorized by experimental approach: Ti implant (n=25), PEEK implant (n=1), cell & cell sheets (n=27), and scaffolds (n=29). Of the 82 included studies, 22 studies were in-vitro, 59 were animal study and only 1 was performed on human participants. 54 articles reported ordered PDL regeneration.

Conclusion: Imaging of this part of the tooth is particularly challenging as it is surrounded by mineralized tissues. Careful selection of sample size, staining protocol and scanning parameter are essential for proper tissue visualization. The knowledge obtained from the different studies which aimed to restore the PDL reflect the need for further experiments to achieve this goal. Deeper understanding of the structural components of the PDL will improve the chances to successfully develop biomimetic dental implants.

Résumé

Contexte: La perte de dents est l'une des maladies bucco-dentaires les plus courantes. Elle est généralement traitée par des prothèses amovibles, fixes ou soutenues par des implants. Bien que les implants dentaires osseointegrés soient une option efficace, ils présentent des lacunes anatomiques, biologiques, physiologiques et mécaniques, principalement en raison de l'absence de ligament parodontal (LPD) autour de l'implant. Cependant, la littérature manque d'une compréhension adéquate du LPD, principalement à cause des difficultés d'imager cette structure en 3D. Il est essentiel sur le plan clinique de restaurer le LPD autour des implants pour améliorer les traitements de la perte dentaire. Une meilleure compréhension du LPD est cruciale pour y parvenir.

Objectifs: i) définir la structure 3D naturelle du LPD à l'aide d'imagerie tomographique nano-computée avec contraste amélioré, et ii) réaliser une revue des recherches sur la création d'implants biomimétiques ou des interfaces entre implants et tissus voisins.

Matériel et Méthodes: Des souris C57Bl/6 (n=5), âgées de 28 à 35 jours, ont été euthanasiées. Dix échantillons de moignon mandibulaire ont été préparés, fixés dans une solution de Bouin pendant 24h, puis stockés au réfrigérateur. Les échantillons ont été colorés avec des agents tels que l'iodure de potassium (IKI), l'acide phosphotungstique (PTA) ou le chlorure de mercure (HgCl), puis montés dans de l'agarose avant numérisation. L'imagerie a été réalisée avec le Zeiss Xradia 520 versa et les images traitées avec Dragonfly. Pour la revue systématique, des bases comme Medline et Embase ont été explorées, et 82 études ont été retenues après un processus de sélection rigoureux. Les critères d'inclusion comprenaient des études in-vivo et in-vitro sur la régénération ou substitution du LPD, et l'utilisation d'échafaudages ou de cellules.

Résultats: Le LPD a été correctement imagé dans les échantillons colorés, mais pas dans ceux non colorés. Les fibres de collagène n'étaient pas visibles, même après coloration. La taille des échantillons doit être réduite pour diminuer le temps de numérisation. Les temps de coloration doivent varier de 24h (IKI) à 48h (PTA, PMA). Le PTA et le PMA ont montré un contraste optimal. Les paramètres de numérisation recommandés sont: tension ≅ 40kV, courant ≅ 70µA, pixel ≤ 0,7µm, grossissement optique à 10X, et un temps d'exposition ≥ 20 secondes.

La revue a identifié 9 562 enregistrements initiaux, dont 82 ont satisfait aux critères d'inclusion. Les études se sont concentrées sur la régénération du LPD (n=77) ou sa substitution (n=5). Les approches expérimentales incluaient des implants en Ti (n=25), PEEK (n=1), cellules et échafaudages (n=27 et n=29 respectivement). Parmi les 82 études, 22 étaient in-vitro, 59 in-vivo et une seule portait sur des humains. 54 études ont documenté la régénération du LPD.

Conclusion: L'imagerie du LPD est difficile à réaliser en raison de sa proximité avec les tissus minéralisés. Il est essentiel de bien choisir la taille des échantillons, le protocole de coloration et les paramètres de numérisation pour une bonne visualisation des tissus. Les recherches sur la régénération du LPD montrent la nécessité d'expériences supplémentaires pour restaurer cette structure et réussir le développement d'implants dentaires biomimétiques.

Acknowledgments:

First and foremost, I would like to express my deepest appreciation to my outstanding mentor, Dr. Elizabeth Zimmermann, for her unwavering guidance, support, understanding, and kindness throughout this journey. Her insightful advice and thoughtful opinions have profoundly influenced my academic progress and have helped steer my research closer to achieving my goals.

I would also like to extend my sincere recognition to my co-supervisor, Dr. Raphael de Souza, for his invaluable input and support throughout this research.

My heartfelt gratitude goes to my wife, whose constant support has been a foundation throughout my years of study and during this research. None of my progress would have been possible without her love, care, and steadfast encouragement.

I am especially grateful to my parents, whose tireless efforts planted the seeds of success deep in my soul.

A special thanks to my friends and colleagues whose contributions were essential to the completion of this work.

I would also like to dedicate this work to my twins, who were born in the midst of this journey. I hope that both my challenges and achievements inspire you to overcome obstacles and pursue success in your own futures.

Contribution of Authors:

Mohamad Alkayyal: Master's candidate: Faculty of Dental Medicine and Oral Health Sciences, McGill University, Montreal (QC), Canada: formulated research objectives, research questions, discussed search strategies, review of existing literature to adjust proposed methodology. In the imaging part: prepared study protocol, participated in animal dissection, sample preparation, sample dimension adjustment, contrast stain selection, imaging protocol, and image visualization. In the scoping review part: prepared review protocol, one of three reviewers in screening of articles for final selection; extracted data, synthesized data, and wrote the thesis.

Aya Rajab: DMD student: Faculty of Dental Medicine and Oral Health Sciences, McGill University, Montreal (QC), Canada; second reviewer in screening of articles.

Kawkab Tahboub: PhD candidate: Faculty of Dental Medicine and Oral Health Sciences, McGill University, Montreal (QC), Canada: helped in data curation for scoping review.

Martin Morris: Liaison Librarian, Schulich Library, McGill University, Montreal (QC), Canada: Aided in the refinement of search strategies and conducted searches.

Raphael de Souza: Associate professor, Faculty of Dental Medicine and Oral Health Sciences, McGill University, Montreal (QC), Canada: Co-supervisor. In the scooping review part: generate research question, guided in data interpretation, and edited the written manuscript.

Elizabeth Zimmermann: Assistant professor, Faculty of Dental Medicine and Oral Health Sciences, McGill University, Montreal (QC), Canada: Supervised the preparation of imaging and review protocols. In the imaging part: performed animal euthanasia, dissection, discussed stain selection and imaging protocol, guided in image visualization with software. In the scoping review part: third reviewer in data extraction, guided in data interpretation and edited the written manuscript.

List of Tables and Appendices:

List of Figures:

List of Abbreviations:

3D	Three dimensional
ACP	American College of Prosthodontics
ACSs	Adipose-derived stromal/stem cells
AH	Alkali heat
APTG-CM	Apical tooth germ conditioning medium
AR	Aya Rajab
ATG	Apical tooth germ
BMSC	Bone marrow stem cells
CBB	Ceramic bovine bone
CDC	Centers for Disease Control and Prevention
CGM	Cementum-impregnated gelatine membrane
CT	Computed tomography
DDM	Decalcified dentine matrix
DFSC	Dental follicle stem cells
DPSC	Dental pulp stem cell
ES	Electrospinning
EVA	Ethylene-co-vinyl alcohol
EZ	Elizabeth Zimmermann
FDP	Fixed dental prosthesis
FeHA	Iron-doped hydroxyapatite
FGF	Fibroblast growth factor
GMSC	Gingival-derived mesenchymal stem cells
HA	Hydroxyapatite
HERS	Hertwig's epithelial root sheath
HgCl	Mercury chloride
HUVEC	Human umbilical vein endothelial cells
IKI	Iodine potassium iodide

LIPUS	Low-intensity pulsed ultrasound
MA	Mohamad Alkayyal
MeSH	Medical Subject Headings
Micro-CT	Micro computed tomography
MM	Martin Morris
Nano-CT	Nano computed tomography
NI	Not investigated
NT	Nanotubes
PAFSC	Periapical follicle stem cells
PCL	Poly (e-caprolactone)
PDL	Periodontal ligament
PDLSC	Periodontal ligament stem cells
PEEK	Polyether ether ketone
PGA	Polyglycolic acid
PLCG	Poly lactide co-glycolide
PLGA	Poly lactic-co-glycolic-acid
PLLA	Poly-L-lactide
PMA	Phosphomolybdic acid
PRF	Platelet rich fibrin
PRISMA	Preferred reporting items for systematic reviews and meta-analyses
PTA	Phosphotungstic acid
RDP	Removable dental prosthesis
SCAP	Stem cells of apical papilla
SHEDs	Stem cells from human exfoliated deciduous teeth
SLA	Sand blasted acid etched
TCP	Tricalcium phosphate
TDM	Treated dentine matrix
TI	Titanium implant
WHO	World Health Organization

Chapter 1. Introduction:

According to the World Health Organization (WHO), tooth loss is the third most prevalent oral disease after dental caries and periodontal diseases (1). Tooth loss occurs because of repetitive cycles of caries, periodontal disease, trauma, orthodontic reasons, and surgical resection (2). Tooth loss has a functional (such as chewing, esthetic, and speech), psychological, and financial impact on affected individuals (1). In addition to the direct cost needed to restore missing teeth, the WHO estimates the global indirect financial burden of edentulism to be around $167 billion which includes productivity lost by affected individuals (3).

Usually, patients with tooth loss receive either a removable dental prosthesis (RDP) (complete or partial), a fixed dental prothesis (FDP), or an implant supported restoration (4). These options have advantages and drawbacks based on each individual case, but they all necessitate proper case selection, subtle treatment planning and dexterous treatment execution (5).

Osseointegrated dental implants are a common and important treatment option to replace one or multiple missing teeth. Osseointegrated implants have good biological outcomes and a high long-term survival rate. However, implants lack certain characteristics of the natural system, such as tooth flexibility and proprioception because they lack a periodontal ligament (PDL) (5-7).

To date, the clinician's toolbox lacks an implant with similar outcomes to the natural tooth (8). Researchers have tried to reproduce or mimic the PDL around dental implants. There is a need to aggregate the knowledge and map the literature in order to move the discipline forward.

Surprisingly, the natural PDL has never been widely visualized and studied in its 3D geometry (9). Different laboratory methods have been used to investigate the PDL including light microscopy, electron microscopy, focused ion beam scanning electron microscopy, and second harmonic generation microscopy (10-12). Recently, some researchers have tried to visualize the PDL in 3D using nano computed tomography (Nano-CT) imaging with varying degree of success (9, 13).

In our approach, the logical sequence to successfully develop an implant with a PDL-like organ is to properly study the PDL first and then try to reproduce or mimic it. To the best of our knowledge, no study used contrast staining to investigate the PDL organ in its anatomical 3D configuration. This project incorporates imaging of the natural tissue structures and investigates current approaches for developing soft tissue interfaces between implants and mineralized tissues.

The objectives of this project are i) to define the PDL's natural 3D structure while in its anatomical position utilizing nano-CT imaging and ii) to perform a scoping review of research areas working towards building biomimetic dental implants and interfaces between dental implants and biological tissues.

Chapter 2 of this thesis provides an in-depth background. Chapter 3 and 4 represent the body of this thesis and discusses the scoping review and the nano-CT imaging respectively in details. Chapter 5 provides a scholarly discussion about the body.

Chapter 2. Literature Review:

Tooth loss

Tooth loss is considered an ending point indicator of life-long dental diseases (14). Tooth loss varies from complete edentulism to a wide range of partial edentulism (single to severe) (1). Complete edentulism is defined as "the physical state of the jaws following removal of all erupted teeth" (15). Partial edentulism is defined as "the absence of some but not all of the natural teeth in a dental arch" (16).

The Centers for Disease Control and Prevention (CDC) estimates the prevalence of complete edentulism among US adults aged 65 or more to reach almost 13% while 48% of adults aged less 65 years had retained a full set of permanent teeth (17, 18). The WHO estimates the global prevalence of complete edentulism among adults aged 20 years or more is around 7%. The prevalence is much higher for adults 60 years or older which is estimated to be around 23% (1).

Some authors have proposed different classification systems for partial and complete edentulism based on the number of remaining teeth (14, 19, 20). The WHO defines severe tooth loss as a person with less than nine remaining teeth in the oral cavity including complete edentulism. For prosthodontic purposes, the American College of Prosthodontics (ACP) has developed classification systems for partial and complete edentulism taking in consideration different variables such as the location and extent of the edentulous zone, condition of the remaining teeth, occlusion, and status of the remaining alveolar bone (15, 16).

Effect of edentulism on bone, esthetics, chewing, and speech.

Tooth loss exerts negative impacts on residual alveolar bone, esthetics, masticatory function, and speech. Reports have determined the greatest amount of bone loss takes place on the horizontal level, mainly on the buccal aspect (21). It is estimated that 50% of bone loss occurs during the first year and two third of this loss occur within the first three months (22). To avoid any hard and soft tissue alteration in the esthetic zone, restorative treatment should be planned prior to extraction especially if immediate or early implant placement is considered (23). Additionally, tooth loss can affect the vertical dimension of occlusion which has evident impact on the facial vertical and anteroposterior dimensions as well as loss of cheeks and lips support (24).

Chewing difficulty is strongly correlated with the number of remaining teeth and their distribution. Favorable tooth distribution is described as functional tooth unit or posterior occlusal pair in which each unit includes two opposite occluding teeth (occlusal pair). Some reports have concluded that acceptable chewing function can be achieved if 20 remaining teeth are present. Other reports emphasized the distribution of remaining teeth, specifying that four occlusal units should be preserved (25).

The oral cavity (including the tongue, lips, hard and soft palate, teeth, and jaws) plays an essential role in phonetics as enunciators and articulators. According to the involved oral anatomical structure, sounds can be classified into four categories: palato-lingual, linguo-dental, labio-dental, and bi-labial. Anterior teeth influence speech through angulation, position (vertical and sagittal), occlusal plane, and lip support. Posterior teeth influence speech through occlusal plane, vertical dimension, and tongue space (26).

Current treatment options to replace missing teeth.

Currently, different options can be utilized to replace missing teeth for partially or completely edentulous patients including implant-supported restorations, FDP, and RDP. The purpose of any prosthetic replacement is to restore biting, chewing, esthetics, and phonetics. Each treatment modality has its usages, drawbacks, advantages, and disadvantages. The indication of each option is highly dependent upon each clinical scenario and the case selection should be customized for each patient (5-7).

FDP is the type of prosthetic treatment that stays permanently in the oral cavity. They can be metallic (precious and non-precious) or non-metallic (ceramics and zirconia) and the material selection should be made depending on the case. It is used in the anterior and posterior region and can provide excellent esthetic and function. It is utilized when there is one abutment from each side of the edentulous ridge with a maximum of two missing teeth replaced. It is contra-indicated when there is a long span edentulous area. It requires mouth preparation of the neighbouring abutments by removing some of the axial and occlusal parts of these abutments to receive the retainer part of the FDP. (6)

RDP is a dental prosthesis that can be removed and worn by the patient (27). It is usually worn during the day and recommended to be removed at night to allow some healing time for the denture bearing tissues (28). It is indicated when other options are not feasible due to technical or financial reasons (5). RDPs are usually easier to fabricate and requires no to minimal mouth preparation (28).

Ancient humans have tried to use dental implants in one way or another. The earliest attempts to replace missing teeth were done using gold wire. Later on, some civilizations tried to use oxen bone and ivory to carve tooth-shaped objects and fix it to the neighbouring teeth using gold wire as a splint to replace missing teeth. The first evidence of osseo-integrated implant goes back to the Mayan population where they used shells to replace missing teeth. In the 18th century, Dr. John Hunter successfully transplanted incompletely developed tooth into the comb of a rooster and observed vascularization growth into the tooth. In the 20th century, the use of different metallic alloys (including titanium alloys) was introduced with variable designs by different clinicians and researchers until the first introduction of the current two stage root-form titanium implant model by Dr. PI Branemark in 1978 (29).

There are four main subgroups of dental implants: subperiosteal, trans-osteal, zygomatic, and endosteal implants. Subperiosteal implants are inspired by denture base design with very limited usages (30). Zygomatic implants are long implants that go all the way from the alveolar ridge to the zygomatic bone. It is indicated for cases with severe atrophy or a defect of the posterior maxilla and usually used in the posterior region along with other implants anterior to the canine to support an FDP (31, 32). The trans-osteal implant penetrates the full thickness of the mandibular bone through both cortical plates and is fixed with pins in the inferior mandibular plate (27).

Endosteal implants are the most widely used implants. They can be further classified into blade and root-form type. The major drawback of blade-type implants is the difficulty to prepare an intra-bony slot resembling a keyway for the blade implant. Root form implants are the golden

standard in implant treatment. Osteotomies are easily prepared with excellent adaptability to Implant surface. Root form implant can be between 3-6 mm diameter and 8-20 mm length. Length and diameter play a critical role in the success and survival of the implants (6).

Root form implant placement can be either one-stage or two-stage. In two stage, two surgeries are required, one to insert the implant and wait for osseointegration then a second entry to do implant un-coverage and placement of healing abutment. In one stage, one surgery is required to insert the fixture and healing abutment at once. According to the level of insertion, implants can be bone level and soft tissue level implants. Implant placement timing can be either immediate, early, or delayed. Immediate placement is where root extraction and fixture placement take place at the same time. In early placement, fixture placement takes place after initial healing and bone formation is evident but incomplete. In delayed placement, fixture is inserted after complete bone healing is observed in the radiograph. (33)

Root form implants can also be classified based on material of manufacturing into titanium, titanium alloys, and zirconia. They all have excellent strength and biocompatibility. Zirconia implants have superior esthetics as they are white in color rather than metallic, but more vulnerable to fixture body fracture (7). Based on implant body and surface design, they can be straight or tapered (which affect insertion difficulty, primary stability, and angulation), threaded or non-threaded (screwed-in or tapped, improve surface contact), hydroxyapatite (HA) coated or non-coated, with variable surface roughness using acid etching and/or sand blasting (7).

Dental implants have three main parts: fixture, abutment, and crown. The fixture has multiple zones including 1) implant connection: the zone where the fixture receives the abutment whether internal or external, locking or non-locking, and it can come with different connector shapes and designs (hex, octagon, morse taper, round, internal grooves, and pin slots). 2) Implant platform: the flat surface part where the abutment will be seated. 3) Fixture body: the part that osseointegrates to the bone. The size and depth of the threads along with the surface texture and pitch size are optimized to maximize fixture to bone contact surface. 4) Cervical collar: smooth part available in soft tissue level implant to facilitate soft tissue adaptation on the fixture surface as well as to prevent bacterial and debris accumulation on this part of the fixture. 5) Healing screw: part covering the internal part of the fixture during the wait time of two-stage placement to prevent inward growth of the soft tissue into the internal part (7).

Osseointegration

The term "osseointegration" was first introduced by Branemark to describe the state of direct functional and structural connection between ordered living bone and the surface of the load-bearing implant (34). It is the final step in the bone healing process around the dental implant. The process starts with the formation of non-osseointegrated woven bone at 6 days after implant placement that continues to grow 7-10 days post-implantation. By the 14^{th} day, bone remodeling replaces woven bone with lamellar bone on the implant surface. Bone continues to grow and mature beyond 60 days of implantation (35).

Various factors (either local or systemic) can enhance or deteriorate osseointegration around dental implants. Local factors include oral hygiene, stability and micromotion, the implant

material, surface topography, surface treatment, surface coating, length and diameter of implant, bone grafting, and growth factors. Systemic factors include medications, chronic diseases like diabetes, age, and smoking. (35, 36)

PDL is an integral part of the natural tissues

The PDL is a specialized soft connective tissue located between the cementum of the teeth and the wall of the bony socket. The PDL forms during the root formation stage -after crown completion- from the developing dental organ. The PDL is formed by the fibroblasts derived from the ectomesenchymal cells within the dental follicle component (10). The process of PDL organ formation proceeds from the cementoenamel junction into apical direction and from the mineralized tissue surface (cementum first followed by bone) toward PDL proper (37). Initially, the ligament space consists of unorganized fiber bundles extending from the mineralized tissues. Then, type I collagen is secreted to connect the fiber bundles from both sides creating an organized PDL (10)

The width of mature PDL is less than half a millimeter (ranges between 100-400 μm) and decreases with aging with the thinnest portion in the middle third of the root (10, 37). The PDL is comprised of cellular and extracellular components predominated by fibroblasts and type I collagen, respectively (10). According to their anatomical location and attachment, the principal fibers of the PDL are classified into six categories namely apical, oblique, horizontal, alveolar crest, transseptal, and dentinogingival fibers (37).

The PDL functions as an attachment apparatus between the tooth and bone. It allows micromovement and absorbs dynamic energy to protect the tooth and bone from forces generated during mastication. The structural existence along with the orientation of the different fibers make up a protective (immunological) barrier against microbes and toxins. It also provides vascularity necessary to preserve the biological function of the PDL organ and the adjoining mineralized tissues such as healing and remodeling. Furthermore, the PDL organ is principally responsible to provide proprioception that is essential to provide positioning and coordinate movements (10).

PDL visualization

Dr. G.V. Black was the first to describe the organizational pattern of the soft collagenous PDL membrane in his book “A study of the histological characters of the periosteum and peridental membrane". He described anatomical and histological structure of the PDL membrane in details including thickness, principal PDL fiber bundles, blood supply, and innervation (38).

Researchers have used different methods to visualize and study the structure of the PDL. In 2D, light microscopy (39) has been extensively used followed by SEM (40). After the specimen is obtained, fixed, and preserved, staining takes place before sectioning or slicing. Then the sample is ready to be visualized. Sectioning can be longitudinal, cross-sectional, or oblique and can take place at different levels of the tooth (apical or coronal, mesial or distal, buccal or lingual). It can also be decalcified or undecalcified with variable thickness (1-100 μm) (39, 40).

To have a better understanding, a 3D imaging techniques were used including FIB/SEM (41) and second harmonic generation imaging (12). These imaging techniques can image 10’s of microns

of depth at a time. Therefore, they are generating a 3D image of just a portion of the PDL. Slicing usually takes place during scanning using microtome. 3D reconstruction of the images and image segmentation and filtering is done using image processing software (12, 41).

Chapter 3. Scoping Review:

Introduction

In the United States (US), more than 150 million people are suffering from tooth loss but only 1 million are getting treatment. In the US, it is estimated that more than 3 million implants were placed in 2019 (42). Globally, the implant market was valued at almost $4.5 billion in 2023 and expected to grow progressively in the following years (6.9% per year) (43). Osseo-integrated dental implants are a common treatment option with a 90% survival rate over 10 years (44). Yet, they have inferior performance compared to natural teeth (8).

Compared to natural teeth, dental implants have anatomical, biological, physiological, and mechanical shortcomings. **Anatomically,** root form dental implants are cylindrical or conical in shape, which does not replicate the multi-rooted nature of teeth or the sophisticated anatomical shape and curvature. Furthermore, osseointegrated dental implants lack periodontal tissue strongly attaching the tooth to the investing bone (45).

Biologically, the PDL act as a tight barrier against microbes and microbial product. The "supracrestal attached tissues" are much weaker in implant and easier to infiltrate. Additionally, the absence of the soft tissue interface leads to reduced vascularity and healing response in the peri-implant area (45, 46).

Physiologically, the PDL allows tooth movement which is essential in micromovements during mastication, orthodontic treatment, and growth in children. The PDL also undergoes remodeling along with the surrounding bone allowing them to adapt to any occlusal changes. More

importantly, the PDL plays a major role in proprioception and protection of teeth and jaws from excessive occlusal forces. The PDL provides feedback information about positioning and magnitude of forces thus plays a key role in force and movement harmony. The lack of PDL around implants diminishes tactile sensitivity and reflex function. This can become a more difficult task when osseointegrated implant are present in both jaws (45).

Mechanically, osseo-integrated dental implant has a direct interface with the jawbone, where functional loading, especially off-axis loading, have long-term destructive effect. In contrast, the PDL acts as a shock absorber to dissipate the cyclic forces of mastication (45).

For anatomical, biological, physiological and mechanical reasons, our area of research aims to develop dental implants with natural tooth properties, such as proprioception, remodeling, and orthodontic movements. Ultimately, the research focuses on the interface between the implant and the bone. A range of methods have been investigated ranging from whole organ regeneration to stem cells to synthetic PDL replacement. Moreover, different substrates have been explored such as titanium implant, dentine, ceramics, and synthetic polymers. It is logical that restoration or regeneration of any of the missing tissue can potentially restore its associated functions. Here, we use a scoping review framework to synthesize the knowledge in this research area (47). The scoping review question is what approaches are used to create a biomimetic implant that can restore soft tissue interface between implant and biological tissues.

Materials and Methods

Protocol and registration

The PRISMA-ScR checklist for scoping reviews was followed (48). A protocol for this scoping review was not registered.

Selection (Inclusion/Exclusion) criteria

Eligibility criteria: The inclusion and exclusion criteria are as follows. The inclusion criteria are i) biologically induced growth of an attachment between bone and biocompatible material (e.g., implant, natural tooth), ii) scaffold or other engineered construct to act as an interface between bone and biocompatible material, iii) in-vivo and in-vitro studies, iv) English language. The exclusion criteria are i) osseo-integration between bone and implant or natural tissue, ii) review articles, iii) case reports, and iv) conference abstracts.

Information sources:

A medical librarian (MM) identified candidate studies by creating a scoping review search strategy for Medline (via Ovid), which is given in **Appendix 1**. The strategy comprised a combination of Medical Subject Headings (MeSH), title/abstract keywords, truncations and Boolean operators, and included the concepts of 'periodontium', 'Biomimetic' and 'Dental Implant'. It was subsequently translated for Embase (via Ovid), Compendex and Scopus. Additional articles were identified by reference tracking.

Four databases were searched: i) Compendex, ii) Embase, iii) Medline, iv) Scopus. The data collection was conducted iteratively (49), and the first search ran from inception - June 2022. Subsequent search iterations, incorporating new terms and refinements noted during screening

and data extraction, were performed in August 2022. Limits were applied with respect to language (English only).

Selection of sources of evidence:

Duplicates were removed using a reference management software (Endnote). The titles and abstracts were screened by at least two blinded reviewers (MA, AY) assigning the inclusion/exclusion criteria using Rayyan (50). Then, full-text articles were screened for eligibility. Disagreements between the reviewers were settled through discussion and involving a third reviewer (EZ).

Data charting process

Data charting was completed in two phases. First, after browsing all included records a single excel sheet was created for data extraction. The proposed items for extraction were discussed between three researchers to determine which data to extract and record. This phase of data charting facilitated the decision making for categorization. In the second phase, a separate excel sheet was created for each category. In addition to the previously extracted data, additional category-specific data were extracted. A single reviewer (MA) has performed all data extraction process.

Data items

In the first phase, extracted data included authors, year of publication, in-vivo or in-vitro study, anatomic location of implantation, brief description of methodology, substrate shape, substrate material and biodegradability, and observed tissue outcomes. In the second phase additional data items included name of category and subcategory, scaffold types, cell types, type of animal, and orientation of the newly formed PDL.

Synthesis of results

The included studies were classified and grouped based on the type of PDL outcomes into substitution and regeneration. Based on fabrication, they were also grouped into 4 major categories and further classified into subcategories. By method of experiments, studies are grouped by cell or scaffold types. They were also grouped based on the presence of ordered PDL in the outcomes. Results are presented in narrative format, tables, and pie charts.

Results

Result of the search

The results of the search are presented in the Prisma flowchart (Fig. 3.1). The electronic and manual search performed in the initial stage yielded 9562 records, of which 772 were identified as duplicates and removed. After screening of titles and abstracts, 8839 articles were found irrelevant and rejected as most of them discussed periodontal tissue regeneration, including alveolar bone, and studies restricted to bone defect management. 451 articles were sought for retrieval, three of them could not be retrieved and were subsequently excluded for this reason. The remaining 448 articles were considered eligible for full-text reading out of which 83 articles satisfied the defined inclusion criteria. Details on excluded studies and reasons for exclusion are illustrated in the PRISMA flowchart.

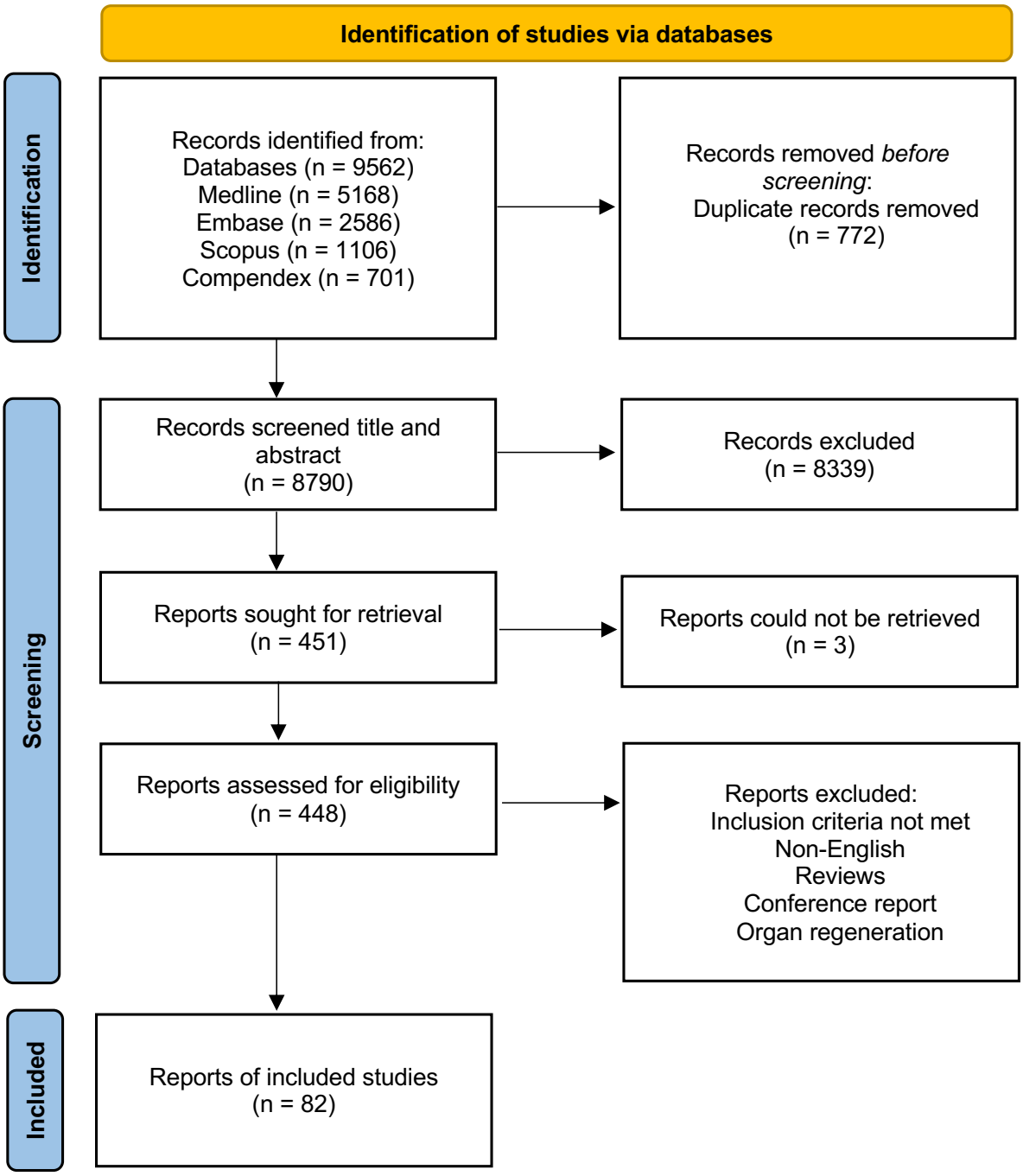

Fig. 3.1 *Prisma flow chart.*

Characteristics of included studies

The included studies were grouped based on the approach used to restore the soft tissue interface, which fell into one of four categories: 1) titanium implants, 2) scaffolds, 3) cells, and 4) polyether ether ketone (PEEK). Based on the PDL outcomes, they were grouped into substitution and regeneration groups. Of the 82 included studies, 22 studies were in-vitro, 59 were animal study and only 1 were performed on human participant (Fig. 3.2).

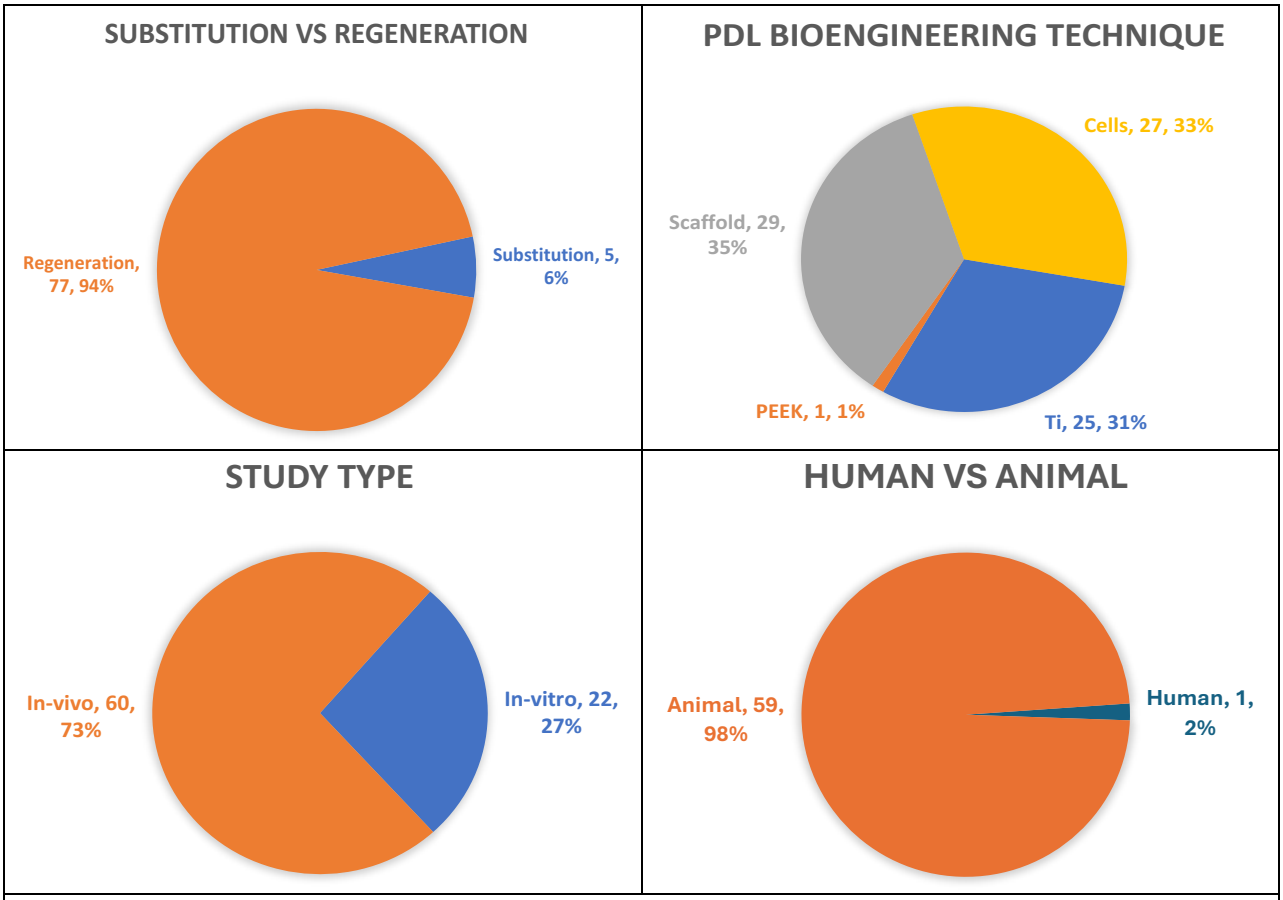

Fig. 3.2. *General characteristics of the included studies*. (Top, left) 94% of the studies sought to regenerate the PDL instead of substituting it for a different material. (Top, right) The approach to regenerate or substitute the PDL was split between purely cellular based approach, use of a scaffold, and use of Titanium implant. Only one study used a PEEK implant. (Bottom, left and right) Most included studies used a pre-clinical in vivo model to test the approach.

Titanium implants (TI)

Of the included studies, 25 articles investigated titanium as the substrate for the bioengineered PDL; the characteristics of these studies are given in Table 3.1. In clinical practice, titanium is a widely used material to replace the tooth root in osseointegrated dental implants. Of the included studies, different approaches were taken to reproduce the effect of the PDL including the following: titanium nanotubes (6 studies), titanium implant combined with a cellular approach (including cell culture, cell sheets, 3D bioprinting, and cell spheroids) (9 studies), and titanium implant combined with a scaffold (10 studies) (Fig. 3.3).

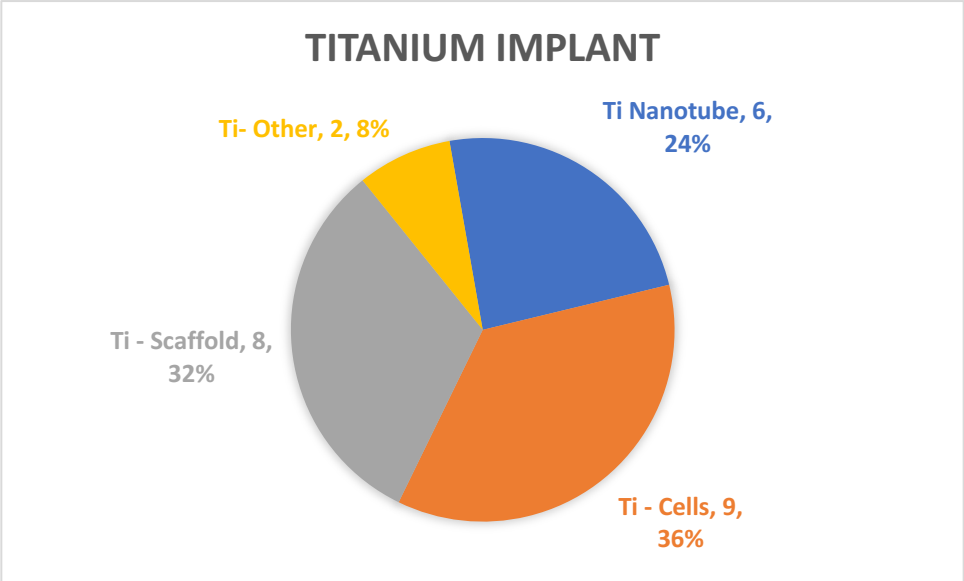

Fig. 3.3. *Ti implant subcategory*: Distribution of approaches to regenerate or substitute the PDL using Ti implants.

Titanium implants with titanium nanotubes (NT): Here, two different approaches were used. One approach formed a titanium nanotube mesh (51) or long nanotubes (52) emanating from a Ti implant. The titanium rods osseointegrated with bone to promote shock absorption between the Ti implant and the alveolar bone. Another approach used nanotubes as short nanorods or

nanospikes to act as loci to initiate collagen production and create bundles in a perpendicular angle (53-56). The later approach was able to produce aligned PDL-like connective tissue (53, 54).

Titanium implants with cells: For the cell technology, nine articles have been identified (three in-vitro and six in-vivo). Six articles have used cell culturing directly on the implant surface using PDL-derived cells (57-61) or dental follicle stem cells (DFSCs) (62). Methods include 3D printing of PDL-derived cells onto the Ti surface (63) as well as single (64) or multi-layered cell sheets (65) on the Ti implant surface. Five of the six in vivo studies reported producing an ordered orientation of the newly bioengineered PDL (perpendicular or angular), while the sixth did not report the orientation of the new collagen bundles. For the in-vitro studies, researchers focused on the ability to regenerate collagen and exhibit cell biomarkers as indicators for successful PDL regeneration. They did not report any physiological alignment of the newly formed collagen bundles, except for one study which reported 3D printing of the cell spheroids around Ti in a tubular pattern (63). Additionally, they did not report any biomechanical properties or in vivo placement under physiological loading.

Titanium implants with scaffolds: Seven articles were identified using different types of scaffolds on titanium as a base for PDL bioengineering (three in-vitro and four in-vivo). The types of materials used for scaffolds include poly (ethylene-co-vinyl alcohol) (EVA), collagen, poly lactide co- glycolide (PLCG), poly (e-caprolactone) (PCL), tricalcium phosphate (TCP), and cementum-impregnated gelatine membrane (CGM). Some articles combined more than one type of scaffold and others combined a scaffold with a cellular approach. Of those, two articles used

EVA as a scaffold supporting gingival cells (66) or periodontal ligaments stem cells (PDLSCs) (67); both approaches reported positive collagen production in vitro as the outcome but failed to report anything about collagen bundle angulation. One article reported using PLCG combined with bone marrow mesenchymal stem cells (BMSC) and reported positive PDL formation perpendicular to the implant surface (68).

Three studies reported using collagen as a scaffold material. The approaches used include 3D bioprinting of PDLSCs and observed PDL formation in vivo (69). The article described the bioprinting to be perpendicular to the implant surface and reported positive PDL formation after implantation. Nonetheless, there is no reporting about the angulation of the newly formed PDL. The second one reported positive PDL formation in a perpendicular angle. They combined TCP with collagen as scaffold and used a mixture of PDLSC and BMSC as cell sheets in vivo (70). The third study combined two types of scaffolds (collagen with PCL) with PDL cell seeding technique and they successfully managed to regenerate an ordered PDL in vitro (71).
Lastly, one article reported using CGM scaffold without cells and reported positive formation of pre-cementum layer (72). They concluded that having cementum deposition will lead to the development of a proper PDL.

Interestingly, Miller et al. (73) reported successful collagen formation in a perpendicular angle in-vitro using nucleation of a functionalized collagen substrate with no use of any cell type. Another in-vivo article reported using bone as a substrate (cementum substitute) by removing the osseointegrated implant along with the attached bone followed by wrapping the implant-bone construct with PDL tissue and replanting it (74). The researchers reported PDL formation at a

perpendicular angle. They also reported a positive response to occlusal stresses, positive neural functions, and positive response to orthodontic movements.

One article reported PDL formation at a perpendicular angle by placing the implant in a hollowed and grooved root (75). The grooves provided a passageway for the PDLCs to reestablish cementum, PDL, and alveolar bone inside this dentine chamber.

Table 3.1. *Study characteristics for studies using Ti implants.* Abbreviations: Ti: titanium, NT: nanotubes, HA: hydroxyapatite, PDLSC: periodontal ligament stem cell, PDL: periodontal ligament, BMSC: bone marrow stem cell, DFSC: dental follicle stem cell, EVA: ethylene-co-vinyl alcohol, CGM: cementum-impregnated gelatine membrane, PCL: poly (e-caprolactone), PLCG: poly lactide co- glycolide, TCP: tricalcium phosphate, AH: alkali heat, HUVEC: human umbilical vein endothelial cells, SLA: sand blasted acid etched, FGF: fibroblast growth factor, NI: not investigated

Authors/ Year	Description of approach		Methodology			Outcomes	
	Technique of interface regeneration	Category	Scaffold	Cell Source	In Vitro/ Animal/ Place of implantation	Characteristics of formed interface or PDL	PDL orientation
Hou et al. 2021 (52)	Ti implant with Ti nanotube array infiltrated with chitosan polymer	Nano Rods	-	-	Rat/femur	TI NT osseointegrate with bone	-
Li et al, 2021 (51)	Ti implant with Ti nanowire scaffold		-	-	In-vitro	Osseointegrated PDL-like Ti NT layer	-
Nojiri et al, 2019 (55)	Ti NT implant/ col linking by electrophoretic fusion and phosphonic acid linker		-	-	In-vitro	Collagen attached to Ti NT protrusion	Perpendicular
Yamada et al, 2016 (56)	Fibroblasts seeded Ti NT micropatterned implant (AH treated)		-	Dermal fibroblast	In-vitro	Collagen production and attachment to spikes	-
Gao et al, 2015 (54)	Ti implant with Ti nanorods/ cell sheets/ HA		-	PDLSCs, BMSCs	Mouse/subcutaneous area	TI NT regenerated new PDL-Cementum layers	Aligned
Kato et al, 2015 (53)	Ti NT implant (AH treated)/ Fibroblast seeding		-	Oral fibroblast	Rabbits/hard palate	PDL formed	Aligned
Ono et al, 2021 (63)	Ti or HA implant - 3D cell printing (tubular)	Cells	-	PDLSCs	In-vitro	Cementum and collagen biomarkers	Tubular printed structure
Washio et al, 2018 (64)	Cell sheet on SLA, CaP coated Ti implants		-	PDLSCs	Rats/femur, dogs/jaw	Cementum and PDL formed	Perpendicular
Lee et al, 2017 (65)	HA coated Ti implant wrapped with 3 layers of cell sheets		-	Cementoblast, PDLCs, HUVEC	Mouse/maxillary first molar	Cementum, PDL, and bone formed	Perpendicular
Oshima et al, 2014 (62)	DF tissue wrapped HA-coated Ti implant		-	DFSC	Mouse/lower molar	Cementum and PDL formed	Perpendicular
Lin et al, 2011 (61)	Matrigel coated then hardened Ti implants. The matrigel is cell seeded		-	PDLSCs	Rats/maxillary molar	Cementum and PDL formed	Perpendicular
Gault et al, 2010 (60)	Cells seeding on TI implants		-	PDLSCs	Mice/subcutaneous, dog/jaw, clinic/human	Cementum and PDL formed	Perpendicular
Kramer et al, 2009 (58)	Micropatterned Ti implant/ integrin mediated cell seeding		-	PDL fibroblast	In-vitro	Cell attachment, collagen formation biomarkers	-
Choi, 2000 (57)	Cells seeding on Ti implants		-	PDLSCs	Dog/jaw	Cementum and PDL formed	Perpendicular
Craig et al, 1999 (59)	Cells seeding on Ti surface		-	PDL, gingival cells	In-vitro	Collagen and cementum	-
Safi et al, 2022 (70)	TCP laser coated Ti or zirconia implant/ 3 layers cell sheets / collagen	Scaffold	TCP-collagen	PDLSCs, BMSCs	Rabbits/jaw-mandibular incisors	PDL formed	Perpendicular
Lee et al, 2021 (69)	3D bioprinting of cell containing collagen-FGF ink on micropatterned Ti implant		Collagen	PDLSCs	Rats/calvaria	PDL formed	-
Ren et al, 2017 (71)	Cell seeded, electrospinning nanopatterned PCL/Collagen fiber on Ti		Collagen-PCL on TI disc	PDLSCs	In-vitro	Collagen	Aligned
Marei et al, 2009 (68)	HA-Ti implant - cells seeded PLCG micropatterned scaffold		PLCG	BMSCs	Goats/jaw	Cementum and PDL formed	Perpendicular
Matsumura et al, 2007 (66)	Ti implant – cell seeded EVA		EVA	Gingival cells	In-vitro	Collagen production	-
Khouw et al, 2001 (67)	Ti implant/ collagen/ EVA/ cell seeding		Collagen/ EVA	PDLSCs	In-vitro	Collagen production	-
Nishimura et al, 1997 (72)	Cementum impregnated gelatin membrane wrapped around HA-coated implant		CGM	-	Monkey/jaw	Precementum	-
Miller et al, 2020 (73)	Functionalized fibers nucleation of collagen monomer fibers on Ti implant		Collagen	-	In-vitro	Collagen fiber	Perpendicular
Nakajima et al, 2016 (74)	PDL tissue wrapped on harvested osseointegrated Ti implant then replanted		Bone	PDL tissues	Rats, mouse/jaw	PDL formed	Perpendicular
Parlar et al, 2005 (75)	Ti implant in hollowed root dentine with side slits		Dentine chamber	-	Dogs	PDL formed	Perpendicular

PEEK

Polyether ether ketone (PEEK) is another common implant material. However, this polymer is not commonly used in dental applications. One study from 2007 used PEEK as a solid substrate to tightly anchor newly formed collagen fibrils (Table 3.2). They used PDL tissue as source of cells and added alkaline phosphatase to induce mineralization at the PEEK-PDL interface to prevent contraction of the collagen bundles and, hence loosening. They reported successful collagen production and stabilization in-vitro but did not report collagen alignment (76). This study is a proof of concept that a system mimicking the natural tissues can be formed to anchor the PDL to the PEEK substrate with mineralization. However, to date, we are unaware of any follow up studies on PEEK.

Table 3.2. Study characteristics for study with PEEK implant. Abbreviation: PEEK: polyether ether ketone, NI: not investigated.

Authors	Technique of interface regeneration	Scaffold	Cell Source	In Vitro Y/N	Outcome	PDL Orientation
Berendsen et al, 2007 (76)	Collagen gel mineralizes at interface with PEEK and in presence of alkaline phosphatase to anchor to PEEK substrate	Collagen	PDL fibroblasts	Y	Collagen	NI

Cells or cell sheets

In the included articles from the search, 27 articles used cells or cell sheets to form a PDL-like interface (Table 3.3). The studies were further divided into four subcategories (as illustrated in Figure 3.4): i) cell homing (1 study), ii) cell seeding (7 studies), iii) cell pellet (5 studies), and iv) cell sheet (14 studies). Over half of the studies took the approach of using a cell sheet.

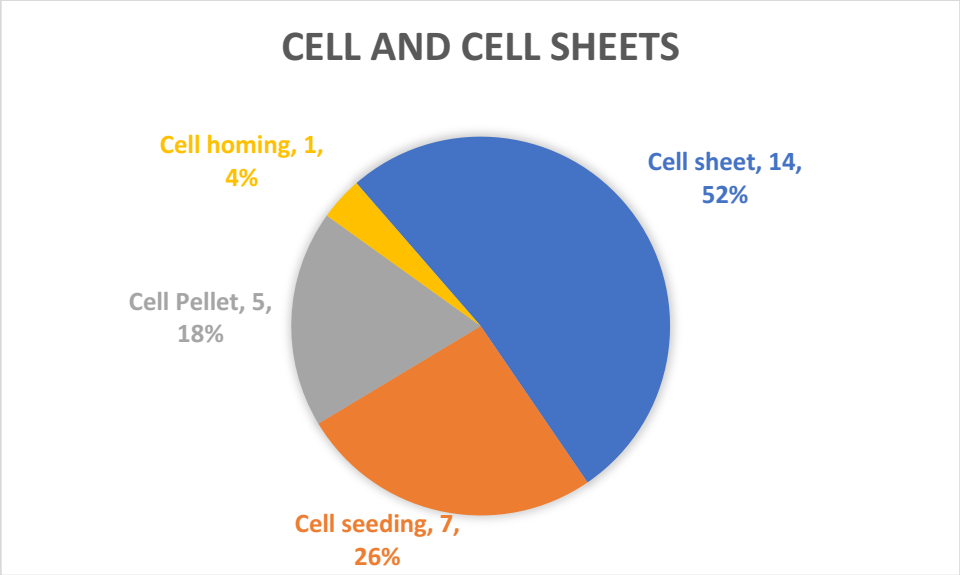

Fig. 3.4. Distribution of cell & cell sheets studies subcategories

Cell homing: Ji et al. (77) reported successful PDL formation in vivo using a cell homing technique and observed angled PDL fibers. They used treated dentine matrix (TDM) with platelet rich fibrin (PRF) to induce PDL formation in a fresh extraction socket. Ankylosis and resorption were reported in the case of late placement.

Cell Seeding: Seven articles were identified implementing cell seeding in-vivo. All articles took place between 2004-2012 and reported formation of new PDLs in a perpendicular angle (78-83) except one article failed to report the angulation of the newly formed PDLs (84). The researchers used different substrates to seed the cells particularly ceramic bovine bone (CBB) (3 studies), treated dentine (1 study), TCP-HA (2 study), and nano-HA modified dentine (1 study). They also utilized different types of cells specifically DFSC, PDLSC, dental pulp stem cell (DPSC), stem cell from apical papilla (SCAP) and BMSC. As signaling factors, Yang et al. (79) reported the use of apical tooth germ conditioning medium for signaling, while Dangaria et al. (81) reported the used of microtopography to drive new PDL production by progenitor cells.

Cell Pellet: Five studies used a cell pellet, which is a mass of cells that secretes a large amount of ECM. Cell pellet can be molded to take the anatomical 3D shape of tooth root. Studies using this process were published between 2008-2014 and all reported new PDL formation in perpendicular angle in-vivo. CBB, dentine, and bone were used as substrates while PDLSC, BMSC, and apical tooth germ (ATG) cells were the used cell types. (85-89). Yang et al reported the use of apical tooth germ conditioning medium (APTG-CM) for cell signaling (85).

Cell Sheet: Fourteen studies were identified under this category between 2008-2021 (11 in-vivo and 3 in-vitro). Cell sheets with three (5 studies), two (1 study), or one (8 studies) layers were investigated. The in-vitro studies only examined cells differentiation, cellular activities, and biomarkers to confirm collagen production. They did not conduct any histological examination to confirm the production and orientation of any new PDL formation. DFSCs, PDLSCs, BMSCs, and HUVECs are the cell types used (90-92).

All in-vivo studies confirmed collagen or PDL production via histological examination. Six of which have confirmed orderly oriented collagen bundles (93-98). HA, dentine, CBB, TCP are the used substrates and PDLSCs, BMSCs, gingival-derived mesenchymal stem cells (GMSCs), ATG cells, DFSCs, Hertwig's epithelial root sheath (HERS) cells, Stem cells from human exfoliated deciduous teeth (SHEDs), and DPSCs are the used cells. One study has reported using APTG-CM as a signaling factor (95). The remaining five in-vivo studies did not describe the orientation of the newly formed PDL (99-103). Dentine, TCP, and HA are the substrates and PDLSCs, osteoblasts, HUVECs, BMSCs, DPSCs, and DFSCs are the used cells.

Table 3.3. Study characteristics for studies only using cells or cell sheets. Abbreviations: PRF: platelet rich fibrin, TDM: treated dentin matrix, DFSC: dental follicle stem cells, PDLSC: periodontal ligament stem cells, DPSC: dental pulp stem cells, BMSC: bone marrow stem cells, PAFSC: periapical follicle stem cells, HA: hydroxyapatite, TCP: tricalcium phosphate, CBB: ceramic bovine bone, APTG-CM: apical tooth germ conditioning medium, HERS: Hertwig's epithelial root sheath, HUVEC: human umbilical vein endothelial cells, SCAP: Stem cells of apical papilla, LIPUS: Low-intensity pulsed ultrasound, GMSC: gingival-derived mesenchymal stem cells, SHEDs: Stem cells from human exfoliated deciduous teeth, NI: implies not investigated in the study.

Author/Year	Description of approach		Methodology		Outcomes	
	Technique of interface regeneration	Cell (# layers)	Cell source	In Vitro/ Animal/ Place of implantation	Formed tissues	PDL orientation
Ji et al, 2015 (77)	PRF wrapped TDM placed in tooth extraction socket	Cell homing	Remaining cells in socket	Dogs/ Jaw	Cementum & PDL formed	Perpendicular
Guo et al, 2012 (84)	DFSCs subclones mixed with CBB powder	Cell seeding	DFSC	Mouse/ Subcutaneous area	PDL formed	NI
Guo et al, 2012 (78)	DFSCs cells on TDM substrate then co-cultured then implanted		DFSCs	Rats/ Omental pouch + Jaw+ Skull	All root tissues formed	Perpendicular
Dangaria et al, 2011 (81)	Seeding of PDL progenitor cells on (nano patterned HA coated or polished substrate)		PDLSCs	Rats/Mouth	Cementum & PDL formed	Perpendicular
Han et al, 2010 (82)	PAFSC cells mixed with CBB powder		PAFSCs, PDLSCs	Mouse, Rats/ Subcutaneous area	Cementum & PDL formed	Perpendicular
Yang et al, 2009 (79)	APTG-CM PDLSC cells mixed with CBB powder		PDLSCs	Mouse/ Subcutaneous area	Cementum & PDL formed	Perpendicular
Sonoyama et al, 2006 (83)	Cells on root-shaped HA-TCP substrate		PDLSCs + SCAP (Human)	Mouse/Subcutaneous area, pig/Jaw	Dentine, PDL, & Cementum	Perpendicular
Seo et al, 2004 (80)	PDLSC cells mixed with HA-TCP particles		PDLSCs, DPSCs (ctrl1) + BMSCs (ctrl2)	Mouse/ Subcutaneous area, Rats/ Jaw	PDL formed	Perpendicular
Guo et al, 2014 (86)	Multilayered PDLSC cell pellet on TDM	Pellet	PDLSCs, fibroblasts	Rats/ Omental pouch + Jaw	PDL formed	Perpendicular
Xie et al, 2012 (87)	Cell pellet from cell sheet of mixed PDLSC and CBB powder		PDLSCs, BMSCs	Mouse/ Subcutaneous area	Cementum & PDL formed	Perpendicular
Bai et al, 2011 (89)	Pellets from Co-cultured cell sheet of DFSCs and HERS		DFSCs, HERS	Rats/ Omental pouch	Cementum & PDL formed	Perpendicular
Yang et al, 2009 (85)	APTG-CM PDLSCs pellet on Dentine and CBB		PDLSC	Mouse/ Subcutaneous area	Cementum & PDL formed	Perpendicular
Li et al, 2008 (88)	Dental papilla cells on millipore transfilter bioengineered dentine block with PDLSCs pellet inside a bone trunk		PDLSCs	Mouse/ Subcutaneous area	Cementum & PDL formed	Perpendicular
Chu et al, 2021 (90)	3 layers DFSCs cell sheets rolled as organoid	Sheet (3)	DFSCs	In Vitro	NI	NI
Safi et al, 2019 (91)	BMSCs and PDLSCc co-cultured into 3 layers cell sheet on collagen membrane		BMSCs, PDLSC	In Vitro	NI	NI
Panduwawala et al, 2017 (101)	HUVECs & PDLSCs co-cultured into 3 layers cell sheet on cementum denuded root		PDLSCs, HUVECs	Mouse/ Subcutaneous area	Collagen	NI
Nagai et al, 2009 (92)	3 layers cell sheet of co-cultured Fibroblasts and HUVECs in Collagen gel		Fibroblasts and HUVECs	In Vitro	NI	NI
Flores et al, 2008 (97)	Fibrin supported 3 layers cell sheets on dentine block		PDLSCs	Rats/ Subcutaneous area	Cementum & PDL formed	Perpendicular
Wang et al, 2016 (102)	PDLSC sheet /PRF/ jaw BMSC sheet on (TDM then TCP+HA)	Sheet (2)	PDLSCs, h jaw BMSCs	Mouse/ Subcutaneous area	PDL formed	NI
Li et al, 2021 (93)	LIPUS irradiated cell sheet wrapped HA substrate	Sheet (1)	PDLSCs	Mouse/ Subcutaneous	PDL formed	Ordered
Raju et al, 2020 (99)	Single cell sheet on extracted tooth root of either types of cells or a sheet of mixed cells		PDLSCs, Osteoblasts	Mouse/ Subrenal capsule + Maxillary molar defect	PDL formed	NI
Meng et al, 2020 (100)	DPSC cell sheet on TDM substrate		DPSCs	Mouse/ Subcutaneous area	All root tissues	NI
Yang et al, 2019 (98)	TDM substrate wrapped with DFSCs or SHEDs cell sheet		DFSCS, SHEDs	Mouse/Subcutaneous area, rats/Jaw	Bone & PDL formation	Perpendicular
Zhang et al, 2016 (94)	PDLSCs & h jaw BMSCs co-cultured cell sheet wrapping TDM or CBB		PDLSCs, h jaw BMSCs	Mouse/ Subcutaneous area	PDL formed	Ordered
Chen et al, 2016 (95)	(APTG-CM) PDLSCs or GMSCs cell sheet on (a dentine layer and outer layer of CBB)		PDLSCs, GMSCs	Mouse/ Subcutaneous area	PDL formed	Ordered
Ji et al, 2013 (96)	Deciduous and permanent teeth PDLSCs cells sheet on TDM		PDLSCs	Mouse/ Peritoneal cavity	PDL formed	Perpendicular
Yang et al, 2012 (103)	DFSC cell sheet wrapping TDM (experimental) or HA/TCP (Ctrl)		DFSCs	Mouse/ Subcutaneous area	All root tissues & non-bundled Collagen	NI

Scaffolds

This is the largest category in our review with twenty-nine studies included (9 in-vitro and 20 in-vivo) conducted between 2006-2023. Scaffolds can be used solo or combined with other scaffolds and they accept all types of cell technologies. They can be layered to produce triphasic, biphasic, or monophasic scaffolds. They can also be used by their own or attached to substrates. Five major types of scaffolds have been retrieved by our search: i) ceramics (5 studies), ii) collagen (6 studies), iii) gelatin (3 studies), iv) poly e-caprolactone (PCL) polymer (14 studies), and v) other polymers (2 studies). Figure 3.5 represents the distribution of included studies in each subcategory.

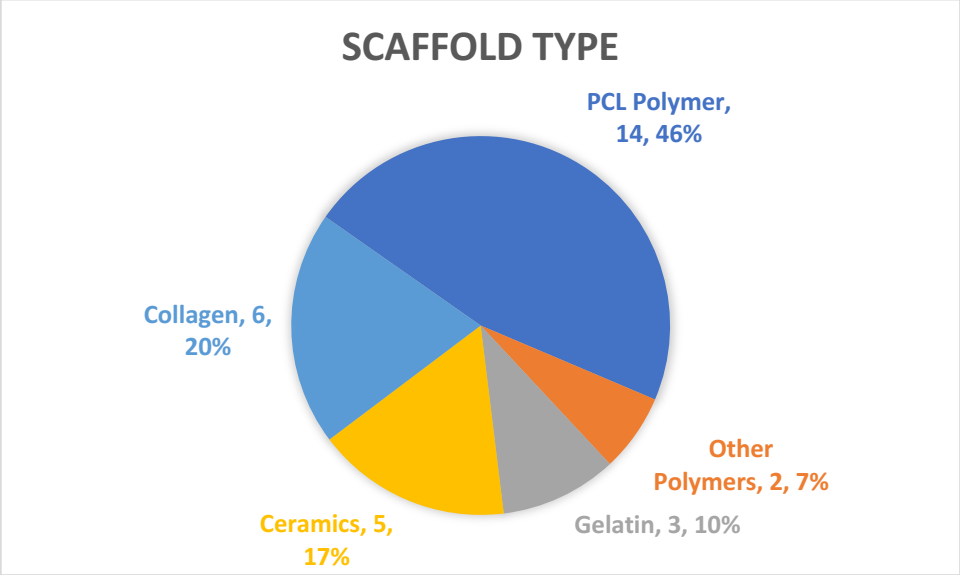

Fig. 3.5. Distribution of scaffolds studies subcategories.

Ceramics: Four articles were retrieved using ceramics as scaffold (all in vivo). Of which, TDM (1 study) combined with ASCS, DFSCs, or SHEDs cells seeding (104), HA-TCP (2 studies) combined with PDLSCs and DPSCs cell sheets (105, 106), decalcified dentine matrix (DDM)

and HA-TCP with DFSC seeding (1 study) (107). All of them confirmed new PDL formation in perpendicular angle except Yuan et al who failed to report the orientation of the new PDL.

Collagen: Six studies were identified using this scaffold (five in-vitro and one in-vivo). Of which collagen only (1) (108), collagen with cells PDLSC (2) (109, 110), collagen with small intestine submucosa and gingival fibroblast cells (1) (111), collagen-poly lactic-co-glycolic-acid (PLGA)-HA and PDLSC and preosteoblasts cells (1) (112), collagen-iron-doped hydroxyapatite (FeHA) and mouse mesenchymal stem cells (1) (113). Two articles (109, 112) aimed to investigate the developed scaffold and reported biomarkers and cell activities and histological analysis of the scaffold without histological examination of any resulting tissues. All the remaining studies reported new formation of PDL with ordered orientation (110, 111, 113) except one that failed to report the orientation of the newly formed PDLs (108).

Gelatin: Three studies were identified under this scaffold type (two in-vivo and one in-vitro), of which gelatin with PDLSC cells (114), gelatin-methacryol-PDLSC & osteoblast cells (115), and gelatin-PLGA-DFSC cells (116). Only one study reported successful new formation of aligned PDL (116). The second study reported successful production of micropatterned scaffold with controlled angulation on topography scaffold imaging (114) while the third study reported failure of formation of any fibrous tissue structure (115).

PCL: 14 studies were included (2 in-vitro and 12 in-vivo), 10 of them PCL with cells only (mainly PDLSC) and 4 combined with other types of scaffolds. The PCL scaffolds were prepared by either 3D printing (9 studies: 8 in-vivo and 1 in-vitro), electrospinning (ES) (4

studies: 3 in-vivo and 1 in vitro), or chemical vapor deposition (1 in vivo). All 3D printed PCL scaffolds reported new PDL formation and ordered alignment (117-124) except one study that failed to report alignment (125). For the ES group, 3 in-vivo studies reported collagen or PDL formation with only two successfully formed properly aligned fibers (126, 127) and one failed to report ordered alignment (128). The remaining ES study was in-vitro and only reported cellular activities and biomarkers (129). One study in the PCL group has used chemical vapor deposition technique and reported ordered PDL formation in-vivo (130).

Other Polymers: Only two studies were retrieved under this category. One study identified in-vivo using polyglycolic acid fiber mesh (*PGA*) as a scaffold combined with PDLSCs and reported new collagen formation but failed to report their orientation (131). The other study identified in-vitro using Poly-L-lactide (*PLLA*) as a scaffold combined with fibroblasts cells and reported fibroblast growth and activities without any further description of histological findings (132).

Table 3.4. Study characteristics for studies using scaffolds. Abbreviations: TDM: treated dentin matrix, DDM: decalcified dentine matrix, ASCs: adipose-derived stromal/stem cells, SHEDs: stem cells from human exfoliated deciduous teeth, SCAP: stem cells of apical papilla, DFSC: dental follicle stem cells, PDLSC: periodontal ligament stem cells, DPSC: dental pulp stem cells, BMSC: bone marrow stem cells, PLGA: poly lactic-co-glycolic-acid, HA: hydroxyapatite, TCP: tricalcium phosphate, CBB: ceramic bovine bone, APTG-CM: apical tooth germ conditioning medium, HERS: Hertwig's epithelial root sheath, HUVEC: human umbilical vein endothelial cells, GMSC: gingival-derived mesenchymal stem cells, ES: electrospinning, NI: implies not investigated in the study.

Authors/ Year	Technique of interface regeneration	Scaffold type/ Fabrication	Cell source	In vitro/ Animal/ Implantation site	Outcome	PDL orientation
Yuan et al, 2022 (104)	Cells seeding on dentine (ultrasonically cleaned root dentine, no pulp or cementum remains)	TDM	ASCS, DFSCs, SHEDs (human)	Mouse/ Subcutaneous area	PDL formation	NI
Feng et al, 2018 (107)	Porous DDM scaffold seeded with hDFSC between HA-TCP (bone layer) and fresh dentine (root layer)	DDM and HA-TCP	Dental follicle cells (Human 3rd molar)	Mouse/ Kidney (renal capsule)	PDL formation	Perpendicular
Gao et al, 2016 (105)	PDLSC Cell sheet wrapped on DPSC seeded (HA-TCP) scaffold	HA-TCP	PDLSCs, DPSCs	Miniature pig/ Healed lower incisors socket	Cementum & PDL formed	Perpendicular
Wei et al, 2013 (106)	DPSC cell seeded root shaped TCP-HA scaffold wrapped with Vit-C treated PDLSC cell sheet	HA-TCP	PDLSCs, DPSC	Miniature pig/ Jaw	Cementum & PDL formed	Perpendicular
Sahbazoglu et al, 2022 (112)	Nanofibrillar and macroporous PLGA scaffold/Collagen/HA seeded with cells, BMP-2	PLGA-Collagen-HA/ ES	PDLSCs (Human), preosteoblast (market)	In Vitro	Biomarkers	NI
Lin et al, 2021 (109)	3D printed microfibrous collagen scaffold + cells seeding	Collagen/3DP	PDLSCs (Human-immortalized).	In Vitro	Cells viability	Perpendicular fiber (scaffold)
Sprio et al, 2018 (113)	Trilayered scaffold of FeHA/collagen (bone), Collagen (PDLs), FeHA/CA (cementum)	FeHA-Collagen/ ES-Magnetization	Mouse mesenchymal stem cells	In Vitro	Collagen fibers	Perpendicular
Lausch et al, 2018 (108)	Trilayered fibrillar collagen scaffold, mineralized (bone) then unmineralized (PDL) then mineralized resembling (cementum)	Collagen/ in-wl;ell mineralization	-	In Vitro	Collagen	NI
Wu et al, 2018 (111)	Cells seeded collagen membrane (PDL layer) between 2 layers of mineralized cells seeded small intestine submucosa	Collagen-Small intestine submucosa	Gingival fibroblasts (dogs)	Dogs/ Jaw	PDL formation	Perpendicular
Kim et al, 2011 (110)	Cells & collagen mixture under shear in bioreactor	Collagen/ shear stress alignment	PDLSCs (Human).	In Vitro	Collagen and cells	Perpendicular
Vurat et al, 2021 (115)	3D bioprinting of hPDLFs in Gel-MA (PDL layer), hOBs in Gel-MA/HAp-MNP (bone layer) in biochip	Gelatin-methacryol, HA-MNPs/ 3DP	PDLSCs, osteoblasts (human).	Rats/ Subcutaneous area	No fibrous tissue formation of any kind	NI
Chen et al, 2015 (116)	Aligned PLGA/Gelatin electrospun sheets, native dental pulp ECM and TDM seeded with DFSC (APES-TDM-DPEM) i	PLGA-Gelatin/ ES, Cells seeding	DFCS (human, swine), Dentine matrix (swine)	Miniature pig/ Jaw	Cementum, PDL, Bone, & Pulp	Perpendicular
Park et al, 2014 (114)	Micropatterned gelatin scaffold (freezcasting) with angle ctrl seeded with cell	Gelatin/ Freeze casting	PDLSCs (Human).	In Vitro	Scaffold shape	Perpendicular on topography scaffold imaging
Daghrery et al, 2023 (117)	Micropatterned PCL spacing100-500mm and 0-90° angulation seeded with PDLSC. Scaffolds treated bone zonal or PDL.	PCL/3DP	PDLSCs (Human).	Rats/ Jaw	Collagen	Ordered
Kim et al, 2021 (118)	3D printed micropatterned scaffold with 0°, 45°, 90° cell seeded	PCL/3DP	PDLSCs (rats)	Rats/ Subcutaneous area	Fibers	Ordered
Safi et al, 2020 (129)	10mm micropatterned scaffold seeded with cells	PCL/ES	PDLSCs (Human).	In Vitro	Cell growth	NI
Yang et al, 2018 (126)	20 layers of aligned nanofiber PCL films packed together with gelatin then seeded with cells	PCL/ES	PDLSCs (Human).	Rats/ Jaw	PDL formation	Perpendicular
Pilipchuk et al, 2018 (130)	Biphasic scaffold, a micropatterned, PLGA/PCL region (PDL) 15mm apart angled to tooth, & amorphous, PCL region (bone)	PCL-PGLA/ chemical vapor deposition	PDLSCs (Human).	Rats/ Jaw	PDL formation	Perpendicular
Park et al, 2017 (119)	3D printed lost wax micropatterned hybrid tri-layered PCL scaffold 0°, 45°, 90° & cells seeding	PCL/ 3DP	PDLSCs (Human).	In Vitro	Collagen	Perpendicular
Pilipchuk et al, 2016 (120)	3D printed micropatterned scaffold, grooves depth and width ctrl over cells seeded dentine block	PCL/ 3DP	PDLSCs (Human)+ fibroblast.	Mouse/ Subcutaneous area	Collagen	Perpendicular
Costa et al, 2014 (127)	Biphasic scaffold, 3D printed angle ctrl\ bone layer coated with CaP and seeded with osteoblasts to an electrospun periodontal layer covered with PDL cell sheets attached to a dentine block	PCL/ ES, 3DP, CaP coating, Cell sheet	PDLSCs, dentine, osteoblasts (sheep).	Rats/ Subcutaneous area	Collagen	Perpendicular
Park et al, 2014 (121)	3D printed micropatterned scaffold (digitally image guided) with ctrl'd pore size & cells seeded	PCL/ 3DP	PDLSCs (Human).	Rats/Jaw	PDL formation	Perpendicular
Lee et al, 2014 (122)	3D printed micropatterned scaffold with ctrl'd pore size seeded with cells	PCL-HA/ 3DP	PDLSCs , Dental pulp stem cells(Human).	Mouse/ Subcutaneous area	PDL formation	Perpendicular
Vaquette et al, 2012 (128)	Osteoblast seed 3D printed PCL-TCP layer (bone) on electro-spun PCL layer covered with PDL cell sheet on dentine slice	PCL/ ES, 3DP, Cell sheet	PDLSCs, dentine, osteoblasts (sheep).	Rats/ Subcutaneous area	Bone, PDL, & cementum	Was not observed
Park et al, 2012 (123)	3D printed (mCT guided) wax mold, Fiber guiding (perpendicular channel) scaffold seeded with cells	PCL/ 3DP	PDLSCs (Human).	Rats/Jaw	PDL formation	Perpendicular
Park et al, 2010 (124)	Micropattern 3D printed wax scaffold PGA (PDL), PCL (bone) seeded with cell on dentine slice	PCL-PGA/ 3DP	PDLSCs, GFB (Human).	Mouse/Subcutaneous, perio defect	Bone, PDL, & cementum	Perpendicular
Kim et al, 2010 (125)	Micropatterned 3D printed root-shaped scaffold strand & pore size 200 mm. SDF1 & BMP7	PCL-HA/ 3DP, Cell Homing	Native surrounding structure	Rats/Subcutaneous area, Jaw	Collagen	NI

Wu et al, 2018 (131)	Porous PGA scaffold seeded with cells	PGA	PDLSCs (Human).	Mouse/ Subcutaneous area	Collagen	NI
Liao et al, 2013 (132)	Cells seeded porous scaffold with ctrl'd pore size	PLLA/ Ammonia modification	HPdLLT+ fibroblasts (human)	In Vitro	Fibroblast growth	NI

Chapter 4. Imaging of PDL soft tissues

Introduction

Imaging of PDL using nano-CT has been lately advocated by many researchers as a revolutionary method to study the PDL organ. It has the capability of obtaining nano-scale images while the object is completely intact (i.e., imaging devoid of any destruction or artifacts related to sample handling, slicing, and processing). Additionally, nano-CT imaging can be utilized to image dynamic objects in their functional position (9, 13).

Nano-CT machines have three main components: x-ray generating source, sample chamber, and image acquisition. The x-ray source focal spot size can be decreased to 400 nm which is essential to produce high resolution images. The sample chamber includes a rotating platform where the sample is mounted and tightly stabilized via a sample holder. The platform can be adjusted in all three axes with a nano-scale accuracy. The acquisition part includes image detector and desktop unit that is used to control the machine and contains image processing software (133, 134).

Different parameters need to be carefully considered to achieve the necessary resolution using nano-CT imaging. This includes voltage, amperage, power, voxel size, optical magnification, number of projections, and exposure time. Voltage setting affects the energy of the x-ray photons thus affect their speed and ability to penetrate objects. Denser material requires higher voltage to image. As a rule, optimal discrimination between dissimilar materials can be achieved by lower voltage (134). Amperage, on the other hand, affects the amount of x-ray photons (i.e. the number of photons) and to lesser extent the energy of the photons. The power of the x ray increases by increasing the voltage or amperage or both (135, 136). Voxel size can vary depending on the

machine specification but generally the smaller the voxel size the better the resolution (135). Increasing optical magnification will enhance the resolution and contrast but it will also increase the imaging time. The same concept can be applied on scanning time and number of exposures (136).

To further improve nano-CT imaging and visualization, some authors have suggested the use of contrast-enhanced nano-CT imaging. Pauwels et al (137) has conducted a thorough exploratory study and investigated 28 contrast agents specifically used for soft tissue visualization (mainly muscle). They investigated different properties of each contrast agent and compared their results. These properties include stability in the sample tissues, depth of penetration, contrast discrimination, acidity.

Based on the work of Pauwels et al., we chose four contrast agents: mercury chloride (HgCl), iodine potassium iodide (IKI), phosphotungstic acid (PTA), and phosphomolybdic acid (PMA) to investigate whether contrast-enhanced nano-CT imaging can be used to visualize the PDL in 3D. Among all four agents, only IKI is not permanently fixed in sample tissues and can be dissolved by immersion in water. The IKI also exhibit the best 24h penetrability followed by PTA then PMA and finally HgCl. Sample size should be carefully considered when using these contrast agents. Regarding the contrast discrimination, PTA showed the highest contrast value followed by PMA then HgCl. These contrasts were able to distinguish different muscles fascicles when other contrasts failed. IKI showed the lowest contrast value among the four. It has been shown that PTA and PMA are strong acids and can dissolve bone structure when used at higher concentration. This could be beneficial when some demineralization is favorable (137).

Materials and Methods

Animal use protocol

C57Bl/6 mice (n = 5) aged 28-35 weeks were euthanized with isofluorane anesthesia followed by cervical dislocation. Mandibles were dissected of soft tissue and separated into hemimandibles. This age range was chosen as Vora et al. (138) have shown that most mandibular growth occurs by the age of 28 weeks in C57Bl/6 mice. Use of animals was approved by the McGill Facility Animal Care Committee (AUP MCGL-8236). Euthanasia was performed in accordance with the relevant guidelines and regulations.

Sample Preparation

Sample preparation steps are described in Fig. 4.1. To obtain a higher resolution, hemi-mandibles were trimmed in the dental lab under x-ray guidance using a straight handpiece and cutting disc under copious water coolant to produce the smallest complete samples which included all molars and around 1 mm of intact bone around the PDL space.

Contrast staining protocol and solutions:

First, the samples were fixed with Bouin's solution for 24 hours. Then, the samples were washed with PBS and stored in PBS in a refrigerator. Second, upon staining, the sample were stained with respective stain (see below) on a nutator. Staining time depends on the size of the sample. Afterward, the samples were washed with PBS for few minutes to remove the excessive staining. Finally, the samples were embedded in 1% agarose inside test tube to stabilize the sample during scan.

Solutions:

1) PMA: 1% PMA in ethanol by dissolving 1g PMA in 100 ml of 70% ethanol. 2) PTA: 1% PTA in ethanol by dissolving 1g PTA in 100 ml of 70% ethanol. 3) IKI: 25% Lugol's solution by diluting 25 ml Lugol's solution in 75 ml distilled water. Lugol's solution consists of 5g I_2, 10g KI in 100 ml distilled water. 4) HgCl: 5% Mercury Chloride by dissolving 5g $HgCl_2$ in 100 ml distilled water.

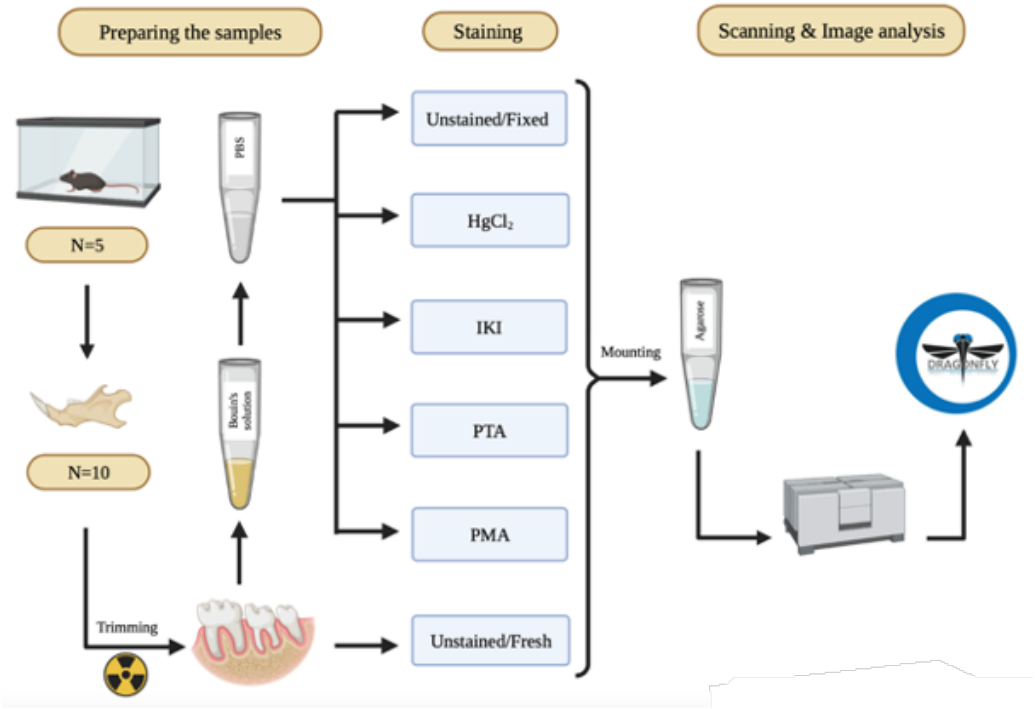

Fig. 4.1 Sample preparation.

Nano-CT imaging

Zeiss Xradia 520 Versa was used at the Integrated Quantitative Biology Initiative at McGill University. Samples were divided into six categories: Scanning parameters were determined

based on literature and modified to fulfil the specific need of scanning soft tissue surrounded by mineralized structure from all aspects (Table 4.1).

Sample	Staining time (days)	kV/uA	Power	Pixel size (microns)	Optical mag	Exposure time (seconds)	Projections
PTA	12	60/83	5	2.6	4x	2	2400
HgCl	23	40/74	3	1	4x	15	1600
IKI	29	40/74	3	1.05	4x	20	1600
PMA	7	40/74	3	0.2	4x	25	659
Fresh	0	40/75	3	0.74	4x	20	1600

Table 4.1 Scanning parameters.

Image Visualization

After image acquisition, images were reconstructed and saved in TIF format. Image analysis software (Dragonfly Workstation, version 2022.2.0.1409, © 2022 Object Research Systems (ORS) Inc.) was used to filter and segment the images.

Results

Here, we present the results of imaging the different contrast-enhanced samples with nano-CT. A 2D slice is shown for each as well as discussion of what structures are visable in the image.

Fresh/Unstained

Fig. 4.2 shows a 3D slice taken of the PDL with nano-CT from a freshly euthanized mouse with no staining of the mandible sample. As can be seen, enamel, dentine, bone, and pulp space are clearly evident, but the PDL cannot be detected as no contrast or radio-opacity within the PDL

space. Only some demarcation lines of blood vessels can be seen in the pulp chamber and inter-radicular area.

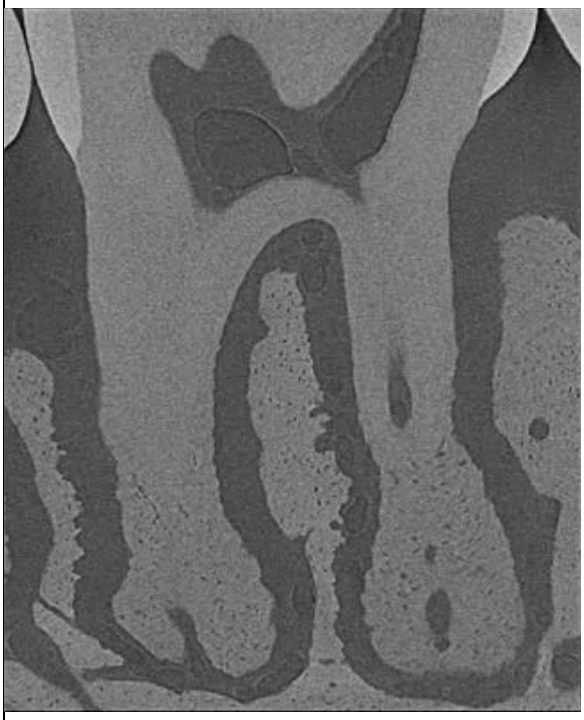

Fig. 4.2 Fresh tissue and unstained.

IKI

Figure 4.3 shows a 2D image from a mandible stained in IKI solution for 29 days. Enamel, dentine, bone, and pulp tissue can be seen. Pulp tissues and PDL tissue can be seen as radio-opaque structures. PDL bundles attachments can be seen especially in the apical area. Staining is overly saturated as evident in the pulp tissue. This has probably caused decrease in contrast. While the PDL are seen in the image, optimization of staining and imaging parameters could further enhance the image visualization. Suggested staining time should not exceed 24 hours as this contrast material has low molecular volume and can easily penetrate the full thickness of the sample within this time frame.

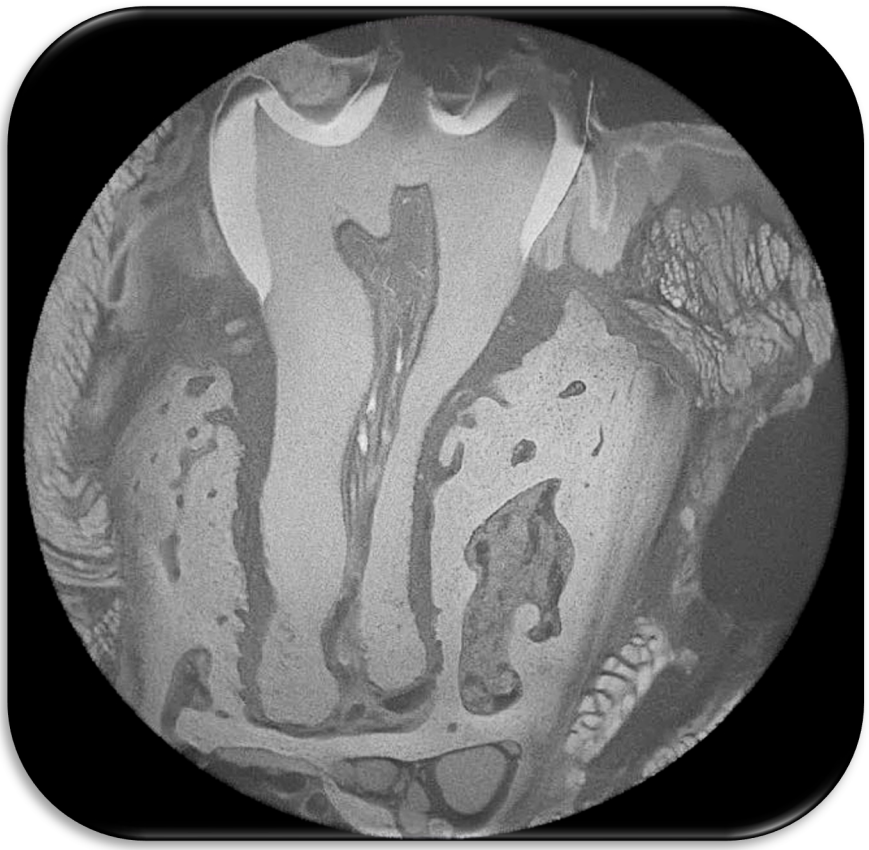

Fig. 4.3 IKI-stained sample.

PTA

Fig. 4.4 shows a sample stained in PTA solution for 12 days. Enamel, dentine, bone, and pulp tissue can be seen. Pulp and PDL tissues are radio-opaque along with the stained jaw muscle fibers. Clearly, this sample is over stained as well. Suggested staining time should not exceed 48 hours. PDL bundles and attachments are seen especially in the apical area.

Fig. 4.4 PTA-stained sample.

PMA

The sample show in Fig. 4.5 was stained in PMA solution for 7 days. Dentine and bone are seen in the apical area. The imaging was off centered which could have caused decrease in focus and resolution. PDL bundles and attachments are seen along with pulp tissue fibers. Staining is also excessive and suggested staining time should not exceed 48 hours.

Fig. 4.5 PMA-stained sample.

HgCl

Fig. 4.6 represent a slice of a sample stained in HgCl for 23 days. Dentine and bone are seen nearly with same contrast. Pulp and PDL tissues look radio opaque with some radiolucent areas reflecting luminal structure. Attachments of the PDL can be seen in the apical area. Staining is very excessive as reflected by the heavily scattered radio opaque deposits. As this material has high molecular weight, staining time should not be exceeding a maximum of 48h.

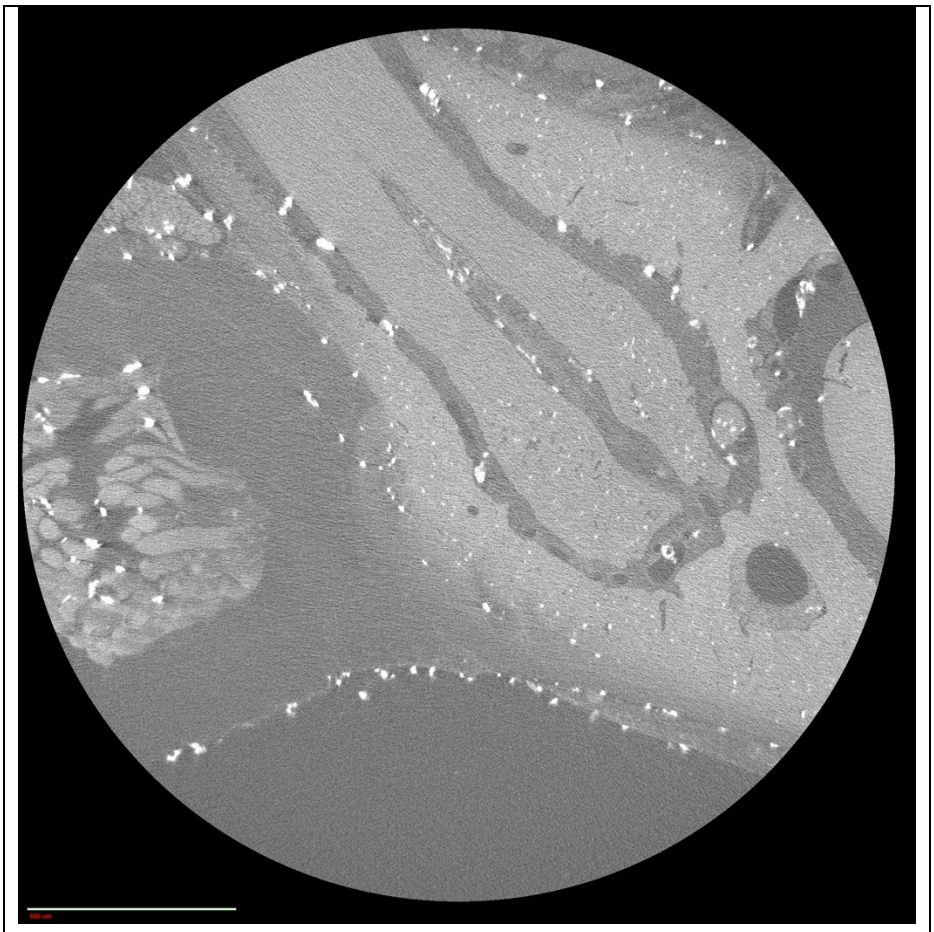

Fig. 4.6 HgCl-stained sample.

Summary

In general, all samples were over stained as there is no previous evidence of such compact tissue surrounded with compact bone. Therefore, it was very difficult to image the PDL tissue even under the used parameters. Staining time should be adjusted between 24h to a maximum of 48h. Exposure parameters should be adjusted to around 40kV and 70μA. Pixel size should be adjusted to 0.7 μm or less and optical magnification should be set at 10X. Exposure time should not be less than 20 seconds. Physical samples size should be drastically minimized to reduce the total imaging time under these parameters.

Chapter 5. Discussion:

The aim of this thesis was to explore what methods have been proposed by different researchers to re-establish through substitution or regeneration the PDL around dental implants and aggregate the included studies to reflect which techniques have more advancements and potentially more relevance at the clinical or laboratory levels. It also aims to visualize the PDL in their anatomical state with contrast enhanced nano-CT imaging.

While nano-CT imaging sounds like an accessible straight forward imaging technique to visualize biological tissues, the size, shape, and structural components of the samples caused difficulty in the imaging process. The needed contrast staining along with proposed exposure parameters would dramatically increase the necessary time to associated cost to image samples. Two groups of researchers (9, 13) have attempted to use nano-CT imaging to visualize PDL without contrast enhancement. While this project could not succeed to surpass or even simulate their work, they both indicated successful imaging of unstained samples with long phase contrast under mechanical loading. Studying the PDL under resting state and during functional loading is a basic step towards any successful design to bioengineer any PDL substitute.

Based on review of the literature and existing publication on the same topic, this scoping review represent an extensive search with 82 articles retrieved. The search strategy and subsequently the retrieved papers of this review focuses only on experimental papers aiming to reproduce or substitute PDL. A subset of the included papers have combined PDL reproduction/substitution along with reproduction/substitution of other tissues such as cementum, bone, and dentine. These papers were included with focus on the PDL reproduction/substitution part particularly in the

classification and data extraction. This scoping review also excluded the excellent work of some researchers who attempted to do whole tooth regeneration, including PDL, in which stem cells were used to reproduce tooth buds that progress through different developmental stages of tooth formation until eruption and root completion (139-142).

Although the use of conventional osseointegrated dental implant successfully restore some of the functions of the missing natural teeth such as chewing, phonetic, and esthetic, the affected individual will still be deprived from other physiological and biological functions such as shock absorption effect of the PDL which can be reflected by energy dissipation or displacement of the root under function, orthodontic tooth movement, response to functional stresses, response to noxious stimuli and pain, proprioception, resistance to microbes and toxins via tight biologic width, and healing capacity (10). Any experimental work to reproduce or substitute PDL should take these factors into account in the evaluation phase to report beneficial and reliable outcomes.

Out of 82 included studies, only 4 studies have partially taken these factors in consideration during their investigations (Table 5.1). All of them are in-vivo and intra-bony (3 jaw and 1 femur). Hou et al. (52) examined the stress dissipation effect of the Ti NT implant compared to the PDL. Under biting, chewing, and occlusion, similar energy dissipation can be seen in both Ti NT implant and natural PDL which is much higher than that of conventional Ti implant. Dangaria et al. (81) applied occlusal displacement forces (10 and 15 NM) on the crowns of both natural teeth and bio-implants and reported similar results. Nakajima et al. (74) and Oshima et al. (62) examined the ability to perform orthodontic movement, response to functional stresses,

response to pain and noxious stimuli, and coordination of movements (proprioception). Both authors have reported similar results when comparing bio-implants to natural teeth.

Table 5.1. Studies with physiological functions reported

Author/Year	Category-Subcategory	Energy dissipation	Displacement	Orthodontic treatment	Functional stresses	Noxious stimuli and pain	Proprioception
Hou et al. 2021 (52)	Ti implant- Nanotube	√					
Nakajima et al, 2016 (74)	Ti Implant-Bone			√	√	√	√
Oshima et al, 2014 (62)	Ti implant-Cells			√	√	√	√
Dangaria et al, 2011 (81)	Cells- seeding		√				

Looking at all approaches together, the studies can be separated into those that regenerate the PDL or those that substitute the PDL. For each approach either substitution or regeneration, many different approaches can reach the same outcome. However, only 5 articles qualify as substitution, while 77 qualify as regeneration (Fig. 3.2).

The approaches used for substitution all use PEEK and titanium, suggesting the possibility to fabricate these types of PDL substitutes outside the recipient body which is supported by the described in vitro fabrication method in each of the five studies. Of those, 3 are titanium nanotube implants (51, 52, 55), 1 titanium-collagen implant (73), and 1 PEEK-collagen implant (76). To narrow down the substitution materials in these five studies, the PDL were substituted either by Ti nanotube (non-biological) or engineered collagen (biological). The Ti nanotube can be osseointegrated directly to the bone or can be attached to the bone by fibrous tissue (mostly short collagen fibers).

The regeneration can also be further subdivided into PDL regeneration, cementum-PDL regeneration, and cementum-PDL-bone regeneration. In the included studies, the researchers attempted to achieve this multilayers regeneration by using multiple layers of cells and cell sheet or scaffolds or mix of both. It is repeatedly reported (26 out of 82) to apply micropattern guidance to direct the angle of growth of the newly regenerated collagen. This micropattern guidance mainly applied with scaffolds, Ti-scaffolds, and Ti nanotube. Other researchers reported the use of conditioning medium, mineralization enhancer or suppressor to direct the regeneration towards mineralized tissues or PDL. Additionally, the use of different kind of cells at different layers affects the direction of regeneration such as the use of fibroblasts versus osteoblasts.

The second classification approach was based on the method of fabrication which resulted in four proposed categories namely titanium implant, PEEK implant, cell & cell sheets, and scaffolds. Further subcategories were proposed under each category (Fig.3.2). Looking at the orientation of PDL outcomes, 54 studies reported ordered outcomes while the remaining studies did not investigate that aspect or reported random fibrous tissue production (Fig. 5.1). All categories have used different types of cells as source of cellular component, when applicable (Fig. 5.2)

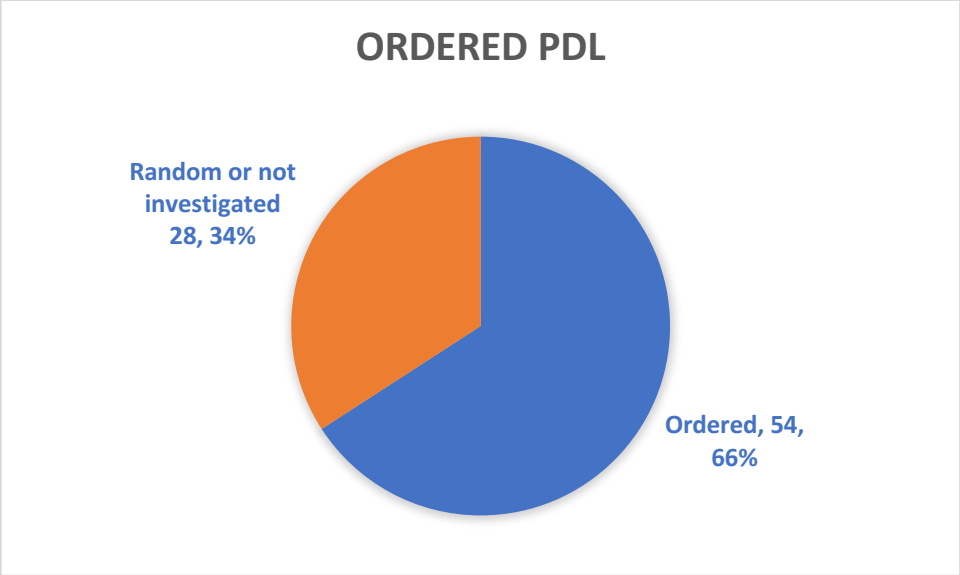

Fig. 5.1. Number and percentage of ordered outcome among included studies

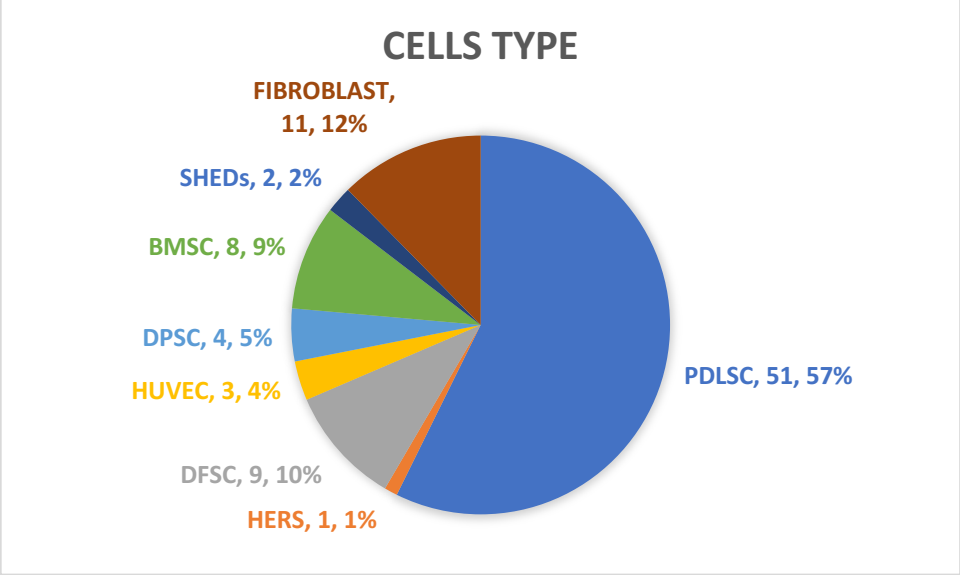

Fig. 5.2. Distribution of cells type among all categories.

In the titanium implant category, nano tube subcategory, the results can be divided into nano tubes study in which the nanotube array osseointegrate with the investing bone giving some flexibility to the implant unit by allowing some micromovement within the limitation of the nano tube. The same can be applied on nanotube mesh surrounding Ti implant. The second approach is to have the long perpendicularly arranged nanotubes attach to the investing bone by short

flexible collagen fibers. The last approach achieved by designing this Ti NT as nano spikes, giving the Ti implant nano pattern to act as loci suitable for collagen bundle to regenerate and attach to these nanospikes; however, further validation is necessary on load-bearing sites.

Parlar et al successfully managed to regenerate PDL around Ti implant in animal model after hollowing out the root removing the pulp and part of dentine and creating internal slits inside this cylindrical investing structure allowing cells to migrate and build PDL around the Ti implant. This suggests the possibility of applying this technique to remaining root cases of single rooted tooth after controlling any preexisting infection.

Nakajima et al used a harvested Ti implant after osseointegration along with the attached bone to act as cementum substitute. The implant-bone unit was wrapped with harvested PDL tissue and replanted on the same location which resulted in perpendicular PDL structure. While this approach sound clinically inacceptable, it utilized the bone as a cementum substitute suggesting the possibility of implementing this technique after customized bone bioengineering in-vitro.

In the Ti implant-cells category, most of the studies used PDLSC or DFSC to initiate the PDL regeneration. 3D cells bioprinting, cell seeding, and cell sheets were used in this Ti implant-cells combination category. Scaffolds were also incorporated under the Ti implant category. Different scaffolds were used combined with cells and cell sheets successfully resulted in the anticipated outcomes.

Miller et al have used different technique with collagen to build up long collagen bundles in a perpendicular angle around Ti implant in vitro. This study suggests the possibility of applying

this technique using a prefabricated Ti implant with PDL substitute. Further experiments are necessary to confirm the outcomes.

Berendsen et al used PEEK implant as a substrate with collagen gel and mineralization technique in vitro to anchor this collagen fibers into the PEEK. While his results do not suggest any possibility for use even in animal model experiment, it opens the door for potential modifications which could lead to a clinically applicable model.

In the cells and cell sheets category, cell homing is applied only in freshly extracted socket which limits the possibility for any future application in immediate implants only. While some of the included studies did not use any solid root shaped substrates, solid root shaped substrate is essential for any clinical application. In the scaffolds category, the PCL represent the main subcategory and includes more sophisticated techniques and components compared to the remaining scaffolds subcategories.

While the vast majority of the included studies did not evaluate the physiological aspect of their results, the Ti implant category included 1 study at the human clinical level and 3 studies with partial physiological testing reported. It also includes 14 intra-bony studies and only 1 extra-bony study which makes it closer to resemble the real-life scenario. Moreover, this category includes almost all of the substitution studies including in-vitro perpendicular nucleation of collagen fibers reflecting the existing and potential experimental advancement in this particular category.

Chapter 6. Conclusion:

In conclusion, from the imaging component, it can be clearly concluded that imaging of this part of the tooth is particularly challenging as it is surrounded by mineralized tissues. Careful selection of sample size, staining protocol and scanning parameter are essential for proper tissue visualization. The knowledge obtained from the different studies which restored periodontal ligaments reflect the ongoing work on this field and the need for further experiments to achieve this goal. Deeper understanding of the structural components of the periodontal ligaments will improve the chances to successfully develop biomimetic dental implants. However, numerous approaches to regenerate or substitute the PDL are promising.

References:

1. Global oral health status report: towards universal health coverage for oral health by 2030: World Health Organization; 2022 [Available from: https://www.who.int/publications/i/item/9789240061484.
2. Peres MA, Macpherson LMD, Weyant RJ, Daly B, Venturelli R, Mathur MR, et al. Oral diseases: a global public health challenge. Lancet. 2019;394(10194):249-60.
3. Jain N, Dutt U, Radenkov I, Jain S. WHO's global oral health status report 2022: Actions, discussion and implementation. Oral Dis. 2024;30(2):73-9.
4. Mark AM. Replacing missing or lost teeth. The Journal of the American Dental Association. 2021;152(5):412.
5. Sather DA, Shillingburg HT. Fundamentals of fixed prosthodontics: Quintessence Publishing Co Ltd; 2012.
6. Rosenstiel SF, Land MF, Fujimoto J. Contemporary fixed prosthodontics. 4th ed. St. Louis, Mo.: Mosby Elsevier; 2006.
7. Misch CE. Contemporary implant dentistry. 3rd ed. St. Louis: Mosby Elsevier; 2008.
8. Pjetursson BE, Heimisdottir K. Dental implants - are they better than natural teeth? Eur J Oral Sci. 2018;126 Suppl 1:81-7.
9. Naveh GR, Brumfeld V, Shahar R, Weiner S. Tooth periodontal ligament: Direct 3D microCT visualization of the collagen network and how the network changes when the tooth is loaded. J Struct Biol. 2013;181(2):108-15.
10. Nanci A, Ten Cate AR. Ten Cate's oral histology : development, structure, and function. 8th ed. St. Louis, Mo.: Elsevier; 2013.
11. Hirashima S, Ohta K, Kanazawa T, Togo A, Kakuma T, Kusukawa J, et al. Three-dimensional ultrastructural and histomorphological analysis of the periodontal ligament with occlusal hypofunction via focused ion beam/scanning electron microscope tomography. Sci. 2019;9(1):9520.
12. Adly MS, Younes R, Martin M, Cloitre T, Adly AS, Panayotov I, et al. New insights in the 3-D rheological properties and collagen fibers orientation in murine periodontal ligaments. Journal of the Mechanics and Physics of Solids. 2024;189:105715.
13. Zhong J, Pierantoni M, Weinkamer R, Brumfeld V, Zheng K, Chen J, et al. Microstructural heterogeneity of the collagenous network in the loaded and unloaded periodontal ligament and its biomechanical implications. J Struct Biol. 2021;213(3):107772.
14. Kassebaum NJ, Bernabé E, Dahiya M, Bhandari B, Murray CJ, Marcenes W. Global Burden of Severe Tooth Loss: A Systematic Review and Meta-analysis. J Dent Res. 2014;93(7 Suppl):20s-8s.
15. McGarry TJ, Nimmo A, Skiba JF, Ahlstrom RH, Smith CR, Koumjian JH. Classification system for complete edentulism. The American College of Prosthodontics. J Prosthodont. 1999;8(1):27-39.
16. McGarry TJ, Nimmo A, Skiba JF, Ahlstrom RH, Smith CR, Koumjian JH, et al. Classification system for partial edentulism. J Prosthodont. 2002;11(3):181-93.
17. Dye BA T-EG, Li X, Iafolla TJ. Dental caries and tooth loss in adults in the United States. Hyattsville, MD: National Center for Health Statistics; 2015.

18. Fleming E AJ, Griffin SO. Prevalence of tooth loss among older adults: United States, 2015–2018. Hyattsville, MD: National Center for Health Statistics; 2020.
19. Nowjack-Raymer RE, Sheiham A. Numbers of natural teeth, diet, and nutritional status in US adults. J Dent Res. 2007;86(12):1171-5.
20. Kassebaum NJ, Smith AGC, Bernabé E, Fleming TD, Reynolds AE, Vos T, et al. Global, Regional, and National Prevalence, Incidence, and Disability-Adjusted Life Years for Oral Conditions for 195 Countries, 1990-2015: A Systematic Analysis for the Global Burden of Diseases, Injuries, and Risk Factors. J Dent Res. 2017;96(4):380-7.
21. Van der Weijden F, Dell'Acqua F, Slot DE. Alveolar bone dimensional changes of post-extraction sockets in humans: a systematic review. J Clin Periodontol. 2009;36(12):1048-58.
22. Schropp L, Wenzel A, Kostopoulos L, Karring T. Bone healing and soft tissue contour changes following single-tooth extraction: a clinical and radiographic 12-month prospective study. Int J Periodontics Restorative Dent. 2003;23(4):313-23.
23. Chappuis V, Araújo MG, Buser D. Clinical relevance of dimensional bone and soft tissue alterations post-extraction in esthetic sites. Periodontol 2000. 2017;73(1):73-83.
24. Craddock HL. Consequences of tooth loss: 1. The patient perspective--aesthetic and functional implications. Dent Update. 2009;36(10):616-9.
25. Naka O, Anastassiadou V, Pissiotis A. Association between functional tooth units and chewing ability in older adults: a systematic review. Gerodontology. 2014;31(3):166-77.
26. Jain CD, Bhaskar DJ, Agali C, Singh H, Gandhi R. Phonetics in dentistry. Int J Dent Med Res. 2014;1(1):31-7.
27. The Glossary of Prosthodontic Terms: Ninth Edition. J Prosthet Dent. 2017;117(5):e1-e105.
28. Carr AB, Brown DT, McCracken WL. McCracken's removable partial prosthodontics. St. Louis, Mo.: Elsevier; 2016. Available from: http://www.dawsonera.com/depp/reader/protected/external/AbstractView/S9780323339919.
29. Abraham CM. A brief historical perspective on dental implants, their surface coatings and treatments. Open Dent J. 2014;8:50-5.
30. Demirdjan E. The complete maxillary subperiosteal implant: an overview of its evolution. J Oral Implantol. 1998;24(4):196-7.
31. Aparicio C, Ouazzani W, Hatano N. The use of zygomatic implants for prosthetic rehabilitation of the severely resorbed maxilla. Periodontol 2000. 2008;47:162-71.
32. Wu Y, Wang F, Huang W, Fan S. Real-Time Navigation in Zygomatic Implant Placement: Workflow. Oral Maxillofac Surg Clin North Am. 2019;31(3):357-67.
33. Koh RU, Rudek I, Wang HL. Immediate implant placement: positives and negatives. Implant Dent. 2010;19(2):98-108.
34. Brånemark PI, Hansson BO, Adell R, Breine U, Lindström J, Hallén O, et al. Osseointegrated implants in the treatment of the edentulous jaw. Experience from a 10-year period. Scand J Plast Reconstr Surg Suppl. 1977;16:1-132.
35. Guglielmotti MB, Olmedo DG, Cabrini RL. Research on implants and osseointegration. Periodontol 2000. 2019;79(1):178-89.
36. Mavrogenis AF, Dimitriou R, Parvizi J, Babis GC. Biology of implant osseointegration. J Musculoskelet Neuronal Interact. 2009;9(2):61-71.

37. de Jong T, Bakker AD, Everts V, Smit TH. The intricate anatomy of the periodontal ligament and its development: Lessons for periodontal regeneration. J Periodontal Res. 2017;52(6):965-74.
38. Black GV. A study of the histological characters of the periosteum and peridental membrane. Chicago: Keener; 1887.
39. Bosshardt DD, Bergomi M, Vaglio G, Wiskott A. Regional structural characteristics of bovine periodontal ligament samples and their suitability for biomechanical tests. Journal of Anatomy. 2008;212(3):319-29.
40. Carter DH, Sloan P. The fibrous architecture of the rat periodontal ligament in cryosections examined by scanning electron microscopy. Arch Oral Biol. 1994;39(11):949-53.
41. Hirashima S, Ohta K, Kanazawa T, Okayama S, Togo A, Miyazono Y, et al. Three-dimensional ultrastructural analysis and histomorphometry of collagen bundles in the periodontal ligament using focused ion beam/scanning electron microscope tomography. J Periodontal Res. 2020;55(1):23-31.
42. THAKKAR R. Trends in Dental Implants 2022: American Academy of Implant Dentistry; 2022 [Available from: https://connect.aaid-implant.org/blog/trends-in-dental-implants-2022#:~:text=In%20the%20US%2C%20more%20than,stronger%20choice%20in%20dental%20restoration.
43. Dental Implants Market Size, Share & Industry Analysis, By Material (Titanium, Zirconium, and Others), By Design (Tapered Implants and Parallel Walled Implants), By Type (Endosteal Implants, Subperiosteal Implants, and Transosteal Implants), By End-user (Solo Practices, DSO/Group Practices, and Others), and Regional Forecast, 2024-2032: Fortunate Business Insight; 2024 [Available from: https://www.fortunebusinessinsights.com/industry-reports/dental-implants-market-100443.
44. Howe MS, Keys W, Richards D. Long-term (10-year) dental implant survival: A systematic review and sensitivity meta-analysis. J Dent. 2019;84:9-21.
45. Newman MG, Klokkevold PR, Elangovan S, Hernandez-Kapila YL, Carranza FA, Takei HH. Newman and Carranza's clinical periodontology and implantology. St. Louis, MO: Elsevier; 2023. Available from: https://www.clinicalkey.com/#!/browse/book/3-s2.0-C20210000225.
46. Dhir S, Mahesh L, Kurtzman GM, Vandana KL. Peri-implant and periodontal tissues: a review of differences and similarities. Compend Contin Educ Dent. 2013;34(7):e69-75.
47. Peters MDJ, Godfrey C, McInerney P, Khalil H, Larsen P, Marnie C, et al. Best practice guidance and reporting items for the development of scoping review protocols. JBI Evid Synth. 2022;20(4):953-68.
48. Tricco AC, Lillie E, Zarin W, O'Brien KK, Colquhoun H, Levac D, et al. PRISMA Extension for Scoping Reviews (PRISMA-ScR): Checklist and Explanation. Ann Intern Med. 2018;169(7):467-73.
49. Morris M, Boruff JT, Gore GC. Scoping reviews: establishing the role of the librarian. J Med Libr Assoc. 2016;104(4):346-54.
50. Ouzzani M, Hammady H, Fedorowicz Z, Elmagarmid A. Rayyan—a web and mobile app for systematic reviews. Systematic Reviews. 2016;5(1):210.
51. Li J, Hua L, Wang W, Gu C, Du J, Hu C. Flexible, high-strength titanium nanowire for scaffold biomimetic periodontal membrane. Biosurface and Biotribology. 2021;7(1):23-9.

52. Hou J, Xiao Z, Liu Z, Zhao H, Zhu Y, Guo L, et al. An Amorphous Peri-Implant Ligament with Combined Osteointegration and Energy-Dissipation. Adv. 2021;33(45).
53. Kato E, Sakurai K, Yamada M. Periodontal-like gingival connective tissue attachment on titanium surface with nano-ordered spikes and pores created by alkali-heat treatment. Dent Mater. 2015;31(5):e116-30.
54. Gao H, Li B, Zhao L, Jin Y. Influence of nanotopography on periodontal ligament stem cell functions and cell sheet based periodontal regeneration. Int J Nanomedicine. 2015;10:4009-27.
55. Nojiri T, Chen C-Y, Kim DM, Da Silva J, Lee C, Maeno M, et al. Establishment of perpendicular protrusion of type i collagen on TiO2 nanotube surface as a priming site of peri-implant connective fibers. J Nanobiotechnology. 2019;17(1).
56. Yamada M, Kato E, Yamamoto A, Sakurai K. A titanium surface with nano-ordered spikes and pores enhances human dermal fibroblastic extracellular matrix production and integration of collagen fibers. Biomed. 2016;11(1):015010.
57. Choi BH. Periodontal ligament formation around titanium implants using cultured periodontal ligament cells: a pilot study. Int J Oral Maxillofac Implants. 2000;15(2):193-6.
58. Kramer PR, Janikkeith A, Cai Z, Ma S, Watanabe I. Integrin mediated attachment of periodontal ligament to titanium surfaces. Dent Mater. 2009;25(7):877-83.
59. Craig RG, LeGeros RZ. Early events associated with periodontal connective tissue attachment formation on titanium and hydroxyapatite surfaces. J Biomed Mater Res. 1999;47(4):585-94.
60. Gault P, Black A, Romette JL, Fuente F, Schroeder K, Thillou F, et al. Tissue-engineered ligament: implant constructs for tooth replacement. J Clin Periodontol. 2010;37(8):750-8.
61. Lin Y, Gallucci GO, Buser D, Bosshardt D, Belser UC, Yelick PC. Bioengineered periodontal tissue formed on titanium dental implants. J Dent Res. 2011;90(2):251-6.
62. Oshima M, Inoue K, Nakajima K, Tachikawa T, Yamazaki H, Isobe T, et al. Functional tooth restoration by next-generation bio-hybrid implant as a bio-hybrid artificial organ replacement therapy. Sci. 2014;4:6044.
63. Ono T, Tomokiyo A, Ipposhi K, Yamashita K, Alhasan MA, Miyazaki Y, et al. Generation of biohybrid implants using a multipotent human periodontal ligament cell line and bioactive core materials. J Cell Physiol. 2021;236(9):6742-53.
64. Washio K, Tsutsumi Y, Tsumanuma Y, Yano K, Srithanyarat SS, Takagi R, et al. In Vivo Periodontium Formation Around Titanium Implants Using Periodontal Ligament Cell Sheet. Tissue Eng Part A. 2018;24(15):1273-82.
65. Lee DJ, Lee JM, Kim EJ, Takata T, Abiko Y, Okano T, et al. Bio-implant as a novel restoration for tooth loss. Sci. 2017;7(1):7414.
66. Matsumura K, Hyon SH, Nakajima N, Tsutsumi S. Effects on gingival cells of hydroxyapatite immobilized on poly(ethylene-co-vinyl alcohol). J Biomed Mater Res A. 2007;82(2):288-95.
67. Peng C, Tsutsumi S, Matsumura K, Nakajima N, Hyon S-H. Morphologic study and syntheses of type I collagen and fibronectin of human periodontal ligament cells cultured on poly(ethylene-co-vinyl alcohol) (EVA) with collagen immobilization. J Biomed Mater Res. 2001;54(2):241-6.

68. Marei MK, Saad MM, El-Ashwah AM, El-Backly RM, Al-Khodary MA. Experimental formation of periodontal structure around titanium implants utilizing bone marrow mesenchymal stem cells: a pilot study. J Oral Implantol. 2009;35(3):106-29.
69. Lee UL, Yun S, Cao HL, Ahn G, Shim JH, Woo SH, et al. Bioprinting on 3D Printed Titanium Scaffolds for Periodontal Ligament Regeneration. Cells. 2021;10(6):28.
70. Safi IN, Hussein BMA, Al-Shammari AM. Bio-hybrid dental implants prepared using stem cells with β-TCP-coated titanium and zirconia. Journal of Periodontal and Implant Science. 2022;52.
71. Ren S, Yao Y, Zhang H, Fan R, Yu Y, Yang J, et al. Aligned Fibers Fabricated by Near-Field Electrospinning Influence the Orientation and Differentiation of hPDLSCs for Periodontal Regeneration. J Biomed Nanotechnol. 2017;13(12):1725-34.
72. Nishimura K, Noguchi Y, Takada K, Suwa K, Imai H. Formation of periodontal ligament-like tissue surrounding cementum-coated hydroxylapatite implants: a pilot study. J N Z Soc Periodontol. 1997(82):11-9.
73. Miller EP, Pokorski JK, Palomo L, Eppell SJ. A Bottom-Up Approach Grafts Collagen Fibrils Perpendicularly to Titanium Surfaces. ACS appl. 2020;3(9):6088-95.
74. Nakajima K, Oshima M, Yamamoto N, Tanaka C, Koitabashi R, Inoue T, et al. Development of a Functional Biohybrid Implant Formed from Periodontal Tissue Utilizing Bioengineering Technology. Tissue Eng Part A. 2016;22(17):1108-15.
75. Parlar A, Bosshardt DD, Unsal B, Cetiner D, Haytac C, Lang NP. New formation of periodontal tissues around titanium implants in a novel dentin chamber model. Clin Oral Implants Res. 2005;16(3):259-67.
76. Berendsen AD, Smit TH, Hoeben KA, Walboomers XF, Bronckers AL, Everts V. Alkaline phosphatase-induced mineral deposition to anchor collagen fibrils to a solid surface. Biomaterials. 2007;28(24):3530-6.
77. Ji B, Sheng L, Chen G, Guo S, Xie L, Yang B, et al. The combination use of platelet-rich fibrin and treated dentin matrix for tooth root regeneration by cell homing. Tissue Eng Part A. 2015;21(1):26-34.
78. Guo W, Gong K, Shi H, Zhu G, He Y, Ding B, et al. Dental follicle cells and treated dentin matrix scaffold for tissue engineering the tooth root. Biomaterials. 2012;33(5):1291-302.
79. Yang ZH, Zhang XJ, Dang NN, Ma ZF, Xu L, Wu JJ, et al. Apical tooth germ cell-conditioned medium enhances the differentiation of periodontal ligament stem cells into cementum/periodontal ligament-like tissues. J Periodontal Res. 2009;44(2):199-210.
80. Seo BM, Miura M, Gronthos S, Bartold PM, Batouli S, Brahim J, et al. Investigation of multipotent postnatal stem cells from human periodontal ligament. Lancet. 2004;364(9429):149-55.
81. Dangaria SJ, Ito Y, Yin L, Valdre G, Luan X, Diekwisch TG. Apatite microtopographies instruct signaling tapestries for progenitor-driven new attachment of teeth. Tissue Eng Part A. 2011;17(3):279-90.
82. Han C, Yang Z, Zhou W, Jin F, Song Y, Wang Y, et al. Periapical follicle stem cell: a promising candidate for cementum/periodontal ligament regeneration and bio-root engineering. Stem Cells Dev. 2010;19(9):1405-15.
83. Sonoyama W, Liu Y, Fang D, Yamaza T, Seo BM, Zhang C, et al. Mesenchymal stem cell-mediated functional tooth regeneration in swine. PLoS ONE. 2006;1:e79.

84. Guo W, Chen L, Gong K, Ding B, Duan Y, Jin Y. Heterogeneous dental follicle cells and the regeneration of complex periodontal tissues. Tissue Eng Part A. 2012;18(5):459-70.
85. Yang Z, Jin F, Zhang X, Ma D, Han C, Huo N, et al. Tissue engineering of cementum/periodontal-ligament complex using a novel three-dimensional pellet cultivation system for human periodontal ligament stem cells. Tissue Eng Part C Methods. 2009;15(4):571-81.
86. Guo W, He Y, Tang X, Chen G, Shi H, Gong K, et al. Scaffold-free cell pellet transplantations can be applied to periodontal regeneration. Cell Transplant. 2014;23(2):181-94.
87. Xie H, Liu H. A novel mixed-type stem cell pellet for cementum/periodontal ligament-like complex. J Periodontol. 2012;83(6):805-15.
88. Li Y, Jin F, Du Y, Ma Z, Li F, Wu G, et al. Cementum and periodontal ligament-like tissue formation induced using bioengineered dentin. Tissue Eng Part A. 2008;14(10):1731-42.
89. Bai Y, Matsuzaka K, Hashimoto S, Fukuyama T, Wu L, Miwa T, et al. Cementum- and periodontal ligament-like tissue formation by dental follicle cell sheets co-cultured with Hertwig's epithelial root sheath cells. Bone. 2011;48:1417-26.
90. Chu J, Pieles O, Pfeifer CG, Alt V, Morsczeck C, Docheva D. Dental follicle cell differentiation towards periodontal ligament-like tissue in a self-assembly three-dimensional organoid model. European Cells and Materials. 2021;42:20-33.
91. Safi IN, Mohammed Ali Hussein B, Al-Shammari AM. In vitro periodontal ligament cell expansion by co-culture method and formation of multi-layered periodontal ligament-derived cell sheets. Regen Ther. 2019;11:225-39.
92. Nagai N, Hirakawa A, Otani N, Munekata M. Development of tissue-engineered human periodontal ligament constructs with intrinsic angiogenic potential. Cells Tissues Organs. 2009;190(6):303-12.
93. Li H, Zhou J, Zhu M, Ying S, Li L, Chen D, et al. Low-intensity pulsed ultrasound promotes the formation of periodontal ligament stem cell sheets and ectopic periodontal tissue regeneration. J Biomed Mater Res A. 2021;109(7):1101-12.
94. Zhang H, Liu S, Zhu B, Xu Q, Ding Y, Jin Y. Composite cell sheet for periodontal regeneration: crosstalk between different types of MSCs in cell sheet facilitates complex periodontal-like tissue regeneration. Stem Cell Res Ther. 2016;7(1):168.
95. Chen Y, Liu H. The differentiation potential of gingival mesenchymal stem cells induced by apical tooth germ cell-conditioned medium. Mol Med Report. 2016;14(4):3565-72.
96. Ji K, Liu Y, Lu W, Yang F, Yu J, Wang X, et al. Periodontal tissue engineering with stem cells from the periodontal ligament of human retained deciduous teeth. J Periodontal Res. 2013;48(1):105-16.
97. Flores MG, Hasegawa M, Yamato M, Takagi R, Okano T, Ishikawa I. Cementum-periodontal ligament complex regeneration using the cell sheet technique. J Periodontal Res. 2008;43(3):364-71.
98. Yang X, Ma Y, Guo W, Yang B, Tian W. Stem cells from human exfoliated deciduous teeth as an alternative cell source in bio-root regeneration. Theranostics. 2019;9(9):2694-711.
99. Raju R, Oshima M, Inoue M, Morita T, Huijiao Y, Waskitho A, et al. Three-dimensional periodontal tissue regeneration using a bone-ligament complex cell sheet. Sci. 2020;10(1):1656.

100. Meng H, Hu L, Zhou Y, Ge Z, Wang H, Wu CT, et al. A Sandwich Structure of Human Dental Pulp Stem Cell Sheet, Treated Dentin Matrix, and Matrigel for Tooth Root Regeneration. Stem Cells Dev. 2020;29(8):521-32.
101. Panduwawala CP, Zhan X, Dissanayaka WL, Samaranayake LP, Jin L, Zhang C. In vivo periodontal tissue regeneration by periodontal ligament stem cells and endothelial cells in three-dimensional cell sheet constructs. J Periodontal Res. 2017;52(3):408-18.
102. Wang ZS, Feng ZH, Wu GF, Bai SZ, Dong Y, Chen FM, et al. The use of platelet-rich fibrin combined with periodontal ligament and jaw bone mesenchymal stem cell sheets for periodontal tissue engineering. Sci. 2016;6:28126.
103. Yang B, Chen G, Li J, Zou Q, Xie D, Chen Y, et al. Tooth root regeneration using dental follicle cell sheets in combination with a dentin matrix - based scaffold. Biomaterials. 2012;33(8):2449-61.
104. Yuan Y, Zhang X, Zhan Y, Tang S, Deng P, Wang Z, et al. Adipose-derived stromal/stem cells are verified to be potential seed candidates for bio-root regeneration in three-dimensional culture. Stem Cell Research and Therapy. 2022;13.
105. Gao ZH, Hu L, Liu GL, Wei FL, Liu Y, Liu ZH, et al. Bio-Root and Implant-Based Restoration as a Tooth Replacement Alternative. J Dent Res. 2016;95(6):642-9.
106. Wei F, Song T, Ding G, Xu J, Liu Y, Liu D, et al. Functional tooth restoration by allogeneic mesenchymal stem cell-based bio-root regeneration in swine. Stem Cells Dev. 2013;22(12):1752-62.
107. Feng G, Wu Y, Yu Y, Huang L, An S, Hu B, et al. Periodontal ligament-like tissue regeneration with drilled porous decalcified dentin matrix sheet composite. Oral Dis. 2018;24(3):429-41.
108. Lausch AJ, Chong LC, Uludag H, Sone ED. Multiphasic Collagen Scaffolds for Engineered Tissue Interfaces. Advanced Functional Materials. 2018;28(48).
109. Lin HH, Chao PG, Tai WC, Chang PC. 3D-Printed Collagen-Based Waveform Microfibrous Scaffold for Periodontal Ligament Reconstruction. Int. 2021;22(14):20.
110. Kim SG, Kim SG, Viechnicki B, Kim S, Nah HD. Engineering of a periodontal ligament construct: cell and fibre alignment induced by shear stress. J Clin Periodontol. 2011;38(12):1130-6.
111. Wu M, Wang J, Zhang Y, Liu H, Dong F. Mineralization Induction of Gingival Fibroblasts and Construction of a Sandwich Tissue-Engineered Complex for Repairing Periodontal Defects. Med Sci Monit. 2018;24:1112-23.
112. Sahbazoglu KB, Demirbilek M, Bayari SH, Buber E, Toklucu S, Turk M, et al. In vitro comparison of nanofibrillar and macroporous-spongious composite tissue scaffolds for periodontal tissue engineering. Connect Tissue Res. 2022;63(2):183-97.
113. Sprio S, Campodoni E, Sandri M, Preti L, Keppler T, Muller FA, et al. A Graded Multifunctional Hybrid Scaffold with Superparamagnetic Ability for Periodontal Regeneration. Int. 2018;19(11):15.
114. Park CH, Kim KH, Rios HF, Lee YM, Giannobile WV, Seol YJ. Spatiotemporally controlled microchannels of periodontal mimic scaffolds. J Dent Res. 2014;93(12):1304-12.
115. Vurat MT, Seker, Lalegul-Ulker O, Parmaksiz M, Elcin AE, Elcin YM. Development of a multicellular 3D-bioprinted microtissue model of human periodontal ligament-alveolar bone

biointerface: Towards a pre-clinical model of periodontal diseases and personalized periodontal tissue engineering. Genes and Diseases. 2021.
116. Chen G, Chen J, Yang B, Li L, Luo X, Zhang X, et al. Combination of aligned PLGA/Gelatin electrospun sheets, native dental pulp extracellular matrix and treated dentin matrix as substrates for tooth root regeneration. Biomaterials. 2015;52:56-70.
117. Daghrery A, Ferreira JA, Xu J, Golafshan N, Kaigler D, Bhaduri SB, et al. Tissue-specific melt electrowritten polymeric scaffolds for coordinated regeneration of soft and hard periodontal tissues. Bioact Mater. 2023;19:268-81.
118. Kim MG, Park CH. Spatial controls of ligamentous tissue orientations using the additively manufactured platforms in an in vivo model: A pilot study. Applied Sciences (Switzerland). 2021;11(17).
119. Park CH, Kim KH, Lee YM, Giannobile WV, Seol YJ. 3D printed, microgroove pattern-driven generation of oriented ligamentous architectures. Int. 2017;18.
120. Pilipchuk SP, Monje A, Jiao Y, Hao J, Kruger L, Flanagan CL, et al. Integration of 3D Printed and Micropatterned Polycaprolactone Scaffolds for Guidance of Oriented Collagenous Tissue Formation In Vivo. Ad. 2016;5(6):676-87.
121. Park CH, Rios HF, Taut AD, Padial-Molina M, Flanagan CL, Pilipchuk SP, et al. Image-based, fiber guiding scaffolds: a platform for regenerating tissue interfaces. Tissue Eng Part C Methods. 2014;20(7):533-42.
122. Lee CH, Hajibandeh J, Suzuki T, Fan A, Shang P, Mao JJ. Three-dimensional printed multiphase scaffolds for regeneration of periodontium complex. Tissue Eng Part A. 2014;20(7):1342-51.
123. Park CH, Rios HF, Jin Q, Sugai JV, Padial-Molina M, Taut AD, et al. Tissue engineering bone-ligament complexes using fiber-guiding scaffolds. Biomaterials. 2012;33(1):137-45.
124. Park CH, Rios HF, Jin Q, Bland ME, Flanagan CL, Hollister SJ, et al. Biomimetic hybrid scaffolds for engineering human tooth-ligament interfaces. Biomaterials. 2010;31(23):5945-52.
125. Kim K, Lee CH, Kim BK, Mao JJ. Anatomically shaped tooth and periodontal regeneration by cell homing. J Dent Res. 2010;89(8):842-7.
126. Yang M, Gao X, Shen Z, Shi X, Lin Z. Gelatin-assisted conglutination of aligned polycaprolactone nanofilms into a multilayered fibre-guiding scaffold for periodontal ligament regeneration. RSC Adv. 2018;9(1):507-18.
127. Costa PF, Vaquette C, Zhang Q, Reis RL, Ivanovski S, Hutmacher DW. Advanced tissue engineering scaffold design for regeneration of the complex hierarchical periodontal structure. J Clin Periodontol. 2014;41(3):283-94.
128. Vaquette C, Fan W, Xiao Y, Hamlet S, Hutmacher DW, Ivanovski S. A biphasic scaffold design combined with cell sheet technology for simultaneous regeneration of alveolar bone/periodontal ligament complex. Biomaterials. 2012;33(22):5560-73.
129. Safi IN, Al-Shammari AM, Ul-Jabbar MA, Hussein BMA. Preparing polycaprolactone scaffolds using electrospinning technique for construction of artificial periodontal ligament tissue. Journal of Taibah University Medical Sciences. 2020;15(5):363-73.
130. Pilipchuk SP, Fretwurst T, Yu N, Larsson L, Kavanagh NM, Asa'ad F, et al. Micropatterned Scaffolds with Immobilized Growth Factor Genes Regenerate Bone and Periodontal Ligament-Like Tissues. Ad. 2018;7(22):e1800750.

131. Wu Y, Xia H, Zhang B, Zhao Y, Wang Y. Assessment of polyglycolic acid scaffolds for periodontal ligament regeneration. Biotechnology and Biotechnological Equipment. 2018;32(3):701-6.
132. Liao W, Okada M, Sakamoto F, Okita N, Inami K, Nishiura A, et al. In vitro human periodontal ligament-like tissue formation with porous poly-L-lactide matrix. Mater Sci Eng C Mater Biol Appl. 2013;33(6):3273-80.
133. Kampschulte M, Langheinirch AC, Sender J, Litzlbauer HD, Althöhn U, Schwab JD, et al. Nano-Computed Tomography: Technique and Applications. Rofo. 2016;188(2):146-54.
134. du Plessis A, Broeckhoven C, Guelpa A, le Roux SG. Laboratory x-ray micro-computed tomography: a user guideline for biological samples. Gigascience. 2017;6(6):1-11.
135. White SC, Pharoah MJ. Oral radiology : principles and interpretation. Edition 7 ed. St. Louis, Missouri: Elsevier; 2014.
136. Bouxsein ML, Boyd SK, Christiansen BA, Guldberg RE, Jepsen KJ, Müller R. Guidelines for assessment of bone microstructure in rodents using micro-computed tomography. J Bone Miner Res. 2010;25(7):1468-86.
137. Pauwels E, Van Loo D, Cornillie P, Brabant L, Van Hoorebeke L. An exploratory study of contrast agents for soft tissue visualization by means of high resolution X-ray computed tomography imaging. J Microsc. 2013;250(1):21-31.
138. Vora SR, Camci ED, Cox TC. Postnatal Ontogeny of the Cranial Base and Craniofacial Skeleton in Male C57BL/6J Mice: A Reference Standard for Quantitative Analysis. Front Physiol. 2015;6:417.
139. Yang KC, Kitamura Y, Wu CC, Chang HH, Ling TY, Kuo TF. Tooth Germ-Like Construct Transplantation for Whole-Tooth Regeneration: An In Vivo Study in the Miniature Pig. Artif Organs. 2016;40(4):E39-50.
140. Kuo TF, Lin HC, Yang KC, Lin FH, Chen MH, Wu CC, et al. Bone marrow combined with dental bud cells promotes tooth regeneration in miniature pig model. Artif Organs. 2011;35(2):113-21.
141. Oshima M, Mizuno M, Imamura A, Ogawa M, Yasukawa M, Yamazaki H, et al. Functional tooth regeneration using a bioengineered tooth unit as a mature organ replacement regenerative therapy. PLoS ONE. 2011;6(7):e21531.
142. Ikeda E, Morita R, Nakao K, Ishida K, Nakamura T, Takano-Yamamoto T, et al. Fully functional bioengineered tooth replacement as an organ replacement therapy. Proc Natl Acad Sci U S A. 2009;106(32):13475-80.

APPENDICES:

Appendix 1. Detailed search strategy:

1. (periodontium or PDL or (periodontal adj5 (ligament? or attach* or regenerat*))).tw,kf.
2. periodont*.sh.
3. exp Periodontal Ligament/ or exp Periodontium/
4. or/1-3
5. exp Biocompatible Materials/
6. exp Biocompatible Materials/ or exp Cell Transplantation/
7. exp Tissue Engineering/ or exp Tissue Scaffolds/
8. ((cell adj3 (stem or trans*)) or biocompatib* or bio-compatib* or biomaterial* or bioartificial* or bio-artificial* or biomanufactur* or bio-manufactur* or hemocompatib* or biomimetic* or bio-mimetic*).tw,kf.
9. or/5-8
10. exp Dental Implants/
11. exp Dental Implantation/
12. Dental Prosthesis/
13. exp Dental Prosthesis/
14. ((implant$ or restor* or rehabilitat*) and (dental* or oral*)).tw,kf.
15. or/10-14
16. 4 and 9
17. 4 and 9 and 15